Theory of high-order harmonic generation by an elliptically polarized laser field

Philippe Antoine,[1,2] Anne L'Huillier,[1,3] Maciej Lewenstein,[1,4] Pascal Salières,[1] and Bertrand Carré[1]
[1]*Commissariat à l'Energie Atomique, DSM/DRECAM/SPAM, Centre d'Etudes de Saclay, 91191 Gif-sur-Yvette, France*
[2]*Laboratoire de Physique Atomique et Moléculaire, Université Catholique de Louvain, Chemin du Cyclotron, 2 B-1348 Louvain-la-Neuve, Belgique*
[3]*Department of Physics, Lund Institute of Technology, S-221 00 Lund, Sweden*
[4]*Centrum Fizyki Teoretycznej, Polska Akademia Nauk, 02-668 Warsaw, Poland*
(Received 10 August 1995)

We generalize a recently formulated theory of high-order harmonic generation by low-frequency laser fields [Anne L'Huillier *et al.*, Phys. Rev. A **48**, R3433 (1993)] to the case of an elliptically polarized light. Our theoretical description includes both the single-atom response and propagation. Phase matching significantly modifies the results obtained in the single-atom response. The results of our calculations, including propagation for both the intensity and polarization properties of harmonics as a function of laser ellipticity, compare very well with recent experimental observations.

PACS number(s): 32.80.Rm, 42.65.Ky

I. INTRODUCTION

High-order harmonic generation (HG) is one of the most rapidly developing topics in the field of intense laser-atom interactions. The recent progress in understanding the origin of the high-order harmonics observed in the experiments (typically beyond the 100th order) [1] can be attributed to the development of the two-step quasiclassical interpretation [2,3]. This model has been very useful in explaining, in particular, the location of the cutoff in the harmonic generation spectra [4]. According to this model, the electron first tunnels [5,6] from the ground state of the atom through the barrier formed by the Coulomb potential and the laser field. Its subsequent motion can be treated classically, and primarily consists in oscillations of the free charge in the laser field. The electron may come back in the vicinity of the nucleus and recombine back to the ground state. If it returns with a kinetic energy $E_{\rm kin}$, a photon of the energy $E_{\rm kin}+I_p$, where I_p is the ionization potential, may be emitted. Since the maximal kinetic energy of the returning electron is $E_{\rm kin}\simeq 3.2U_p$, where $U_p=E^2/4\omega^2$ is the ponderomotive potential, i.e., the mean kinetic energy acquired by a free electron in the laser field of amplitude E and frequency ω, the cutoff in the harmonic spectrum occurs at harmonics of order $N_{\rm max}\simeq(I_p+3.2U_p)/\omega$ [7].

In a series of papers [8,9], we have formulated a fully quantum theory, valid in the tunneling limit ($U_p\geqslant I_p>\omega$), which recovers the semiclassical picture of the two-step model and includes rigorously the effects of quantum tunneling, quantum diffusion, and interference. This theory is a version of the so-called strong-field approximation [5] and is very much related to the δ-potential model of Becker and co-workers [10]. Moreover, we have shown that a single-atom description is not sufficient, in general, to explain the experimental data [8,11]. To get good agreement between theory and experiment, it is necessary to consider the effects of propagation and phase matching of the harmonics in the macroscopic medium. This, to a large extent, is caused by the variation of the harmonic phase, which is due to the phase shift of the fundamental beam at the focus and to the dynamical phase shift of the induced atomic dipole moment [8,11–13].

The two–step model, as well as our theory, lead to the obvious conclusion that HG should be greatly reduced if the atoms are driven by elliptically polarized light. In the case of linear polarization, some of the classical trajectories of the electron pass the nucleus periodically, thus allowing for recombination and harmonic generation. There are, strictly speaking, no such trajectories for elliptic polarization. HG is, in that case, possible only thanks to the finite extent of the electronic wave packet and quantum diffusion effects. The HG efficiency is expected to decrease rapidly with an increase of the ellipticity of the laser. Several laboratories have demonstrated this effect experimentally [14–17]. Measurements have been performed both at relatively low intensities and harmonic orders, i.e., in the multiphoton regime, and at high intensities and harmonic orders, for which the two-step description applies. The decrease of HG strength with ellipticity is clearly more pronounced in the latter case.

Harmonics generated by single atoms driven by elliptically polarized light are also polarized elliptically. In the perturbative regime, their polarization is expected to be the same as that of the laser [18]. This prediction is not valid in the general (nonperturbative) case. Weihe *et al.* [19] have observed that the polarization ellipse of low-order harmonics is rotated by some angle with respect to the polarization ellipse of the laser.

A systematic theoretical study of HG, including the case of elliptically polarized laser fields, has been recently presented by Becker *et al.*, who discussed the exact solutions for the δ-potential model [10]. Dietrich *et al.* [15] used a simplified version of our theory (in which the electron is allowed to return to the nucleus only once) to interpret their experimental data. However, none of these authors discusses propagation effects and the polarization properties of the harmonics, which are the main subject of the present work. Other studies of harmonics generated by laser fields of variable polarization have concentrated on the possibility of gen-

erating attosecond pulses [20], and on applications for control and optimization of the harmonic source using several colors [21,22].

The aim of the present paper is to generalize and apply the theory formulated in Refs. [8,9] to the case of elliptically polarized light. The paper is organized as follows. In Sec. II, we discuss the single-atom response. We show that the variation of the harmonic strengths as a function of laser ellipticity exhibit quantum interference effects, which depend on the laser intensity and harmonic order. In Sec. III, we present the method for calculating the macroscopic response by solving the inhomogeneous Maxwell equations [23] and we compare the propagated results with experimental data [14]. We obtain a very good agreement between theory and experiment. Finally, in Sec. IV, we discuss the polarization of harmonics from the single atom to the macroscopic response. For single atoms, a simple linear dependence of the ellipticity of the harmonics and of the rotation angle of the ellipse as a function of laser ellipticity occurs only at relatively low intensities. For higher intensities, both ellipticity and rotation angle vary rapidly as a function of both laser intensity and ellipticity, and exhibit quantum interference effects. In some situations, the *helicity* of the harmonic field undergoes dynamically induced change of sign, so that, in the complex plane, the fundamental and harmonic fields circulate in opposite directions. All these effects are smoothed (but not eliminated) by propagation effects.

II. SINGLE-ATOM RESPONSE

A. Theory

We consider an atom in a single-electron approximation under the influence of the laser field $\vec{\mathcal{E}}(t)$ of arbitrary polarization. We here use atomic units, but express all energies in terms of the photon energy. A more appropriate system of units (MKSA) will be used in Sec. III to describe the propagation of electromagnetic fields. We skip the details of the derivation and the discussion of the validity range of our approach since they were thoroughly discussed in Ref. [9]. Briefly, we neglect the contribution to the evolution of the system of all bound states except the ground state, as well as the effect of the atomic potential on continuum electronic states. Our approach is valid in the tunneling regime for ionization, i.e., when U_p is comparable or larger than I_p.

The time-dependent dipole moment $\vec{x}(t) = \langle \Psi(t) | \vec{x} | \Psi(t) \rangle$, with $|\Psi(t)\rangle$ denoting the time-dependent electronic wave function, can be written in the form of a generalized Landau-Dyhne formula [24] as

$$\vec{x}(t) = i \int_0^t dt' \int d^3\vec{p}\, \vec{d}^*(\vec{p} - \vec{A}(t)) a^*(t) \times \exp[-iS(\vec{p},t,t')] \vec{\mathcal{E}}(t') \cdot \vec{d}(\vec{p} - \vec{A}(t')) a(t') + \text{c.c.} \tag{1}$$

In this expression, $\vec{d}(\vec{p} - \vec{A}(t))$ is the field-free dipole transition matrix element between the ground-state and the continuum state characterized by the velocity $\vec{v} = \vec{p} - \vec{A}(t)$, $\vec{p}$ denoting the canonical momentum and $\vec{A}(t)$, the vector potential. $a(t)$ is the ground-state amplitude; Finally, $S(\vec{p},t,t')$ is the *quasiclassical action*, describing the motion of an electron moving in the laser field with a constant momentum $\vec{p}$,

$$S(\vec{p},t,t') = \int_{t'}^{t} dt'' \left(\frac{[\vec{p} - \vec{A}(t'')]^2}{2} + I_p \right). \tag{2}$$

Equation (1) is a sum of probability amplitudes corresponding to the following processes: The last term in the integral, $\vec{\mathcal{E}}(t') \cdot \vec{d}(\vec{p} - \vec{A}(t')) a(t')$, is the probability amplitude for an electron to make the transition to the continuum at time t' with the canonical momentum $\vec{p}$. The electronic wave function is then propagated until time t and acquires a phase factor equal to $\exp[-iS(\vec{p},t,t')]$. The electron recombines at time t with an amplitude equal to $\vec{d}^*(\vec{p} - \vec{A}(t)) a^*(t)$. The expression (1) neglects continuum-continuum contributions to $\vec{x}(t)$.

The ground-state amplitude $a(t)$ can be expressed as

$$a(t) = \exp\left(- \int_0^t \gamma(t'') dt'' \right), \tag{3}$$

where the time-dependent, complex, ionization rate is determined from

$$\gamma(t) = \int_0^t dt' \int d^3\vec{p}\, \vec{\mathcal{E}}^*(t) \cdot \vec{d}^*(\vec{p} - \vec{A}(t)) \times \exp[-iS(\vec{p},t,t')] \vec{\mathcal{E}}(t') \cdot \vec{d}(\vec{p} - \vec{A}(t')). \tag{4}$$

For small t, $\gamma(t)$ is a rather complicated function of time, but becomes periodic typically after a few laser cycles. Since the effect of depletion over the time scale of few optical periods is negligible, and since the integral over t' is actually restricted to $t' \simeq t$ owing to quantum diffusion, we may set $a(t') \simeq a(t)$ in Eq. (1).

The harmonic amplitudes $\vec{x}_q$ are obtained by Fourier transforming the time-dependent dipole moment $\vec{x}(t)$:

$$\vec{x}_q = \frac{1}{2\pi} \int_0^{2\pi} \vec{x}(t) e^{iqt} dt. \tag{5}$$

As we have shown in Ref. [9], the dominant contributions to $\vec{x}_q$ come from the stationary points of the Legendre-transformed quasiclassical action, for which the derivatives of $S(\vec{p},t,t') - qt$ with respect to $\vec{p}$, t, and t' vanish (saddle-point equations). Introducing the return time $\tau = t - t'$, these equations read

$$\vec{\nabla}_{\vec{p}} S(\vec{p},t,\tau) = \vec{p}\,\tau - \int_{t-\tau}^{t} \vec{A}(t'') dt'' = \vec{0}, \tag{6}$$

$$\frac{\partial S(\vec{p},t,\tau)}{\partial \tau} = \frac{[\vec{p} - \vec{A}(t-\tau)]^2}{2} + I_p = 0, \tag{7}$$

$$\frac{\partial S(\vec{p},t,\tau)}{\partial t} = \frac{[\vec{p} - \vec{A}(t)]^2}{2} - \frac{[\vec{p} - \vec{A}(t-\tau)]^2}{2} = q. \tag{8}$$

The first of these equations means that the only relevant electron trajectories are those in which the electron leaves the nucleus at time $t-\tau$ and returns to it at t. Equation (7) has a somewhat more complicated interpretation. If I_p was zero, it would simply state that the electron leaving the nucleus at $t-\tau$ should have a velocity equal to zero. In reality, $I_p \neq 0$ and, in order to tunnel through the Coulomb barrier, the electron must have a negative kinetic energy at $t-\tau$. This condition cannot be fulfilled for real τ's, but can easily be fulfilled for complex τ's. The imaginary part of τ can then be interpreted as a tunneling time, just as it has been done in the seminal papers of Ammosov, Delone, and Krainov [6]. Finally, we can rewrite the last expression (8) as

$$\frac{[\vec{p}-\vec{A}(t)]^2}{2}+I_p=E_{\rm kin}(t)+I_p=q. \tag{9}$$

This is simply the energy conservation law, which gives the final kinetic energy of the recombining electron that generates the qth harmonic.

In Ref. [15], such a quasiclassical analysis was used. The authors considered, however, the contribution from only one saddle point $(\vec{p},t,\tau)$, and calculated it in the limit $I_p \ll U_p$. There are, however, in general, several complex stationary points that fulfill the saddle-point equations. In Ref. [12], we included the contribution of the two most relevant saddle points. We showed the importance of interferences between the contributions of these two saddle points at high laser intensities, in the case of linear polarization. In the present paper, we will only use the saddle-point technique to evaluate the integral over momenta, and to handle the slowly varying parts of expression (1), as discussed below. We perform all other integrations over t' (replaced, in practice, by $\tau=t-t'$) and t numerically, thus accounting for the contributions of all saddle points and their interferences exactly. As we shall see, for small ellipticities and moderate intensities, our results for the ellipticity dependences of the harmonics are consistent with those of Ref. [15]. However, for high intensities corresponding to the plateau region (e.g., $>2\times10^{14}$ W/cm^2 for the 43rd harmonic in neon) [12], the interference of the two saddle points that have return times $\mathrm{Re}(\tau)$ in the interval $[0,2\pi]$ becomes very significant. Moreover, for large ellipticities, the contributions of saddle points with even larger return times can no longer be neglected.

After performing the saddle-point integration over momenta in Eq. (1) [see Eq.(6)], replacing $a(t')$ by $a(t)$, and using the return time τ, we obtain

$$\vec{x}(t)=i\int_0^\infty d\tau\left(\frac{\pi}{\nu+i\tau/2}\right)^{3/2}\vec{d}^*(\vec{p}_s-\vec{A}(t)) \times\exp[-iS(\vec{p}_s,t,\tau)]\vec{\mathscr{E}}(t')\cdot\vec{d}(\vec{p}_s-\vec{A}(t-\tau)) \times|a(t)|^2+\text{c.c.}, \tag{10}$$

where ν is a positive regularization constant, whereas

$$\vec{p}_s=\vec{p}_s(t,\tau)=\int_{t-\tau}^{t}dt''\vec{A}(t'')/\tau. \tag{11}$$

Note the characteristic prefactor $(\nu+i\tau/2)^{-3/2}$ coming from the effect of quantum diffusion. It cuts off very efficiently the contributions from large τ's and allows us to extend the integration range from 0 to infinity.

The complex decay rate may be treated in a similar way and becomes

$$\gamma(t)=\int_0^\infty d\tau\left(\frac{\pi}{\nu+i\tau/2}\right)^{3/2}\vec{\mathscr{E}}^*(t)\cdot\vec{d}^*(\vec{p}_s-\vec{A}(t)) \times\exp[-iS(\vec{p}_s,t,\tau)]\vec{\mathscr{E}}(t')\cdot\vec{d}(\vec{p}_s-\vec{A}(t-\tau)). \tag{12}$$

Within this approximation, $\gamma(t)$ is a periodic function of time. Oscillations of $\gamma(t)$ modify obviously the Fourier spectrum of $\vec{x}(t)$, i.e., influence the harmonic spectrum [25]. We have checked numerically, however, that, in the discussed regime of parameters, this effect is negligible. It is thus legitimate to replace $\gamma(t)$ by its time average $\bar{\gamma}$ and to assume that the decay of the ground state is exponential: $|a(t)|^2=\exp(-\Gamma t)$, with $\Gamma=2\,\mathrm{Re}(\bar{\gamma})$. Note that Γ is a function of I_p, U_p, and the polarization of the laser field.

We are now in the position to evaluate the harmonic spectrum emitted by an atom driven by an elliptically polarized field. The laser electric field and vector potential are given by

$$\vec{\mathscr{E}}(t)=\sqrt{\frac{4U_p}{1+\epsilon^2}}(\cos(t),\epsilon\sin(t),0), \tag{13}$$

$$\vec{A}(t)=\sqrt{\frac{4U_p}{1+\epsilon^2}}(-\sin(t),\epsilon\cos(t),0), \tag{14}$$

where ϵ denotes the ellipticity of the laser field.

For the case of hydrogenlike atoms and transitions from s states, the field-free dipole matrix elements can be approximated by [9,26]

$$\vec{d}(\vec{p})=i\frac{2^{7/2}\alpha^{5/4}}{\pi}\frac{\vec{p}}{(\vec{p}^{\,2}+\alpha)^3}, \tag{15}$$

with $\alpha=2I_p$. Many qualitative and some quantitative properties of the HG spectra can be obtained from the simplified expression

$$\vec{d}(\vec{p})\propto\vec{p}. \tag{16}$$

This expression describes a ''flat'' dipole moment and neglects the energy dependence of $\vec{d}(\vec{p})$. It corresponds to the ''Gaussian broad limit'' (GBR) model discussed in Ref. [9]; an analogous formula has been used in Ref. [15]. We stress that our present calculations indicate that the expression (16) cannot be used for accurate quantitative evaluation of the HG spectra. The absolute values of the harmonic strengths and ionization rates from the (appropriately normalized) GBR model are typically two orders of magnitude smaller than those obtained with Eq. (15) [27]. The GBR model does, however, provide quite an accurate description of the relative harmonic intensity and ellipticity dependences.

In the present work, we use Eq. (15). For the term $\vec{d}(\vec{p}_s-\vec{A}(t))$ in Eq. (10), we make use of the fact that the main contribution to the integral over τ and t in the equation

giving the qth harmonic amplitude [Eq. (5), in which $\vec{x}(t)$ is replaced by the expression (10)], comes from the saddle points. We therefore substitute $\{[\vec{p}_s-\vec{A}(t)]^2+\alpha\}^{-3}$ by $(2q)^{-3}$, in accordance with Eqs. (7) and (8). This cannot be done for $\vec{d}(\vec{p}_s-\vec{A}(t-\tau))$, since this term is singular at the saddle point [see Eq. (7)]. We have to treat this term in the integrand of (10) exactly. To this aim, we use the Fourier expansion

$$\frac{1}{\{[\vec{p}_s-\vec{A}(t-\tau)]^2+\alpha\}^3}=\sum_{M=-\infty}^{\infty} b_M(\tau)\exp[-iM(2t-\tau)]. \tag{17}$$

The coefficients $b_M(\tau)$ can be evaluated exactly using the Cauchy theorem, as described in Appendix A.

Without depletion, the Fourier transform of $\vec{x}(t)$[Eq. (5)] consists of a series of the Dirac's δ peaks. The moduli squared of these amplitudes determine the corresponding harmonic strengths. With depletion, the Fourier transform of $\vec{x}(t)$ becomes a sum of Lorentzian peaks centered at the harmonic frequencies. In the present regime of parameters, these peaks are still very narrow, since $\Gamma \ll 1$. Note that this condition means that depletion is negligible on a scale of one laser cycle, which does not exclude that it might be dominant on a scale of the laser pulse duration, T_D. The complex harmonic amplitudes are calculated as the values of the Fourier transform of $\vec{x}(t)$ at the centers of the lines, i.e., at the harmonic frequencies, multiplied by appropriate normalization factors N. The normalization is such that $|N|^2$ gives the total area under the corresponding Lorentzian peak in the spectrum (total energy emitted into the given harmonic field), i.e., $N^2=(1-e^{-2\Gamma T_D})/2\Gamma$.

The final expressions for the x and y components for the complex harmonic amplitudes read

$$x_q=N\sum_{M=-\infty}^{\infty}\int_0^{\infty} d\tau X_{K-M}(\tau)b_M(\tau)e^{iM\tau}, \tag{18}$$

$$y_q=N\sum_{M=-\infty}^{\infty}\int_0^{\infty} d\tau Y_{K-M}(\tau)b_M(\tau)e^{iM\tau}, \tag{19}$$

where $2K=q-1$,

$$\begin{aligned}X_K(\tau)=i\left(\frac{U_p}{(1+\epsilon^2)}\right)^{3/2}\frac{32\alpha^{5/2}}{\pi^2(2K+1)^3}(i)^K\left(\frac{\pi}{\nu+i\tau/2}\right)^{3/2}\exp[-iF_K(\tau)][-(1-\epsilon^2)B(\tau)J_{K+2}(\tilde{U}_pC(\tau))\\ -i(1-\epsilon^2)e^{i\tau}B(\tau)J_{K-1}(\tilde{U}_pC(\tau))+i[(1+\epsilon^2)e^{i\tau}B(\tau)+D(\tau)+i\epsilon^2C(\tau)]J_{K+1}(\tilde{U}_pC(\tau))+\{(1+\epsilon^2)B(\tau)\\ +[D(\tau)-i\epsilon^2C(\tau)]e^{i\tau}\}J_K(\tilde{U}_pC(\tau))],\end{aligned} \tag{20}$$

$$\begin{aligned}Y_K(\tau)=i\left(\frac{U_p}{(1+\epsilon^2)}\right)^{3/2}\frac{32\alpha^{5/2}}{\pi^2(2K+1)^3}(i)^K\frac{\epsilon}{i}\left(\frac{\pi}{\nu+i\tau/2}\right)^{3/2}\exp[-iF_K(\tau)][-(1-\epsilon^2)B(\tau)J_{K+2}(\tilde{U}_pC(\tau))\\ +i(1-\epsilon^2)e^{i\tau}B(\tau)J_{K-1}(\tilde{U}_pC(\tau))+i[(1+\epsilon^2)e^{i\tau}B(\tau)+\epsilon^2D(\tau)+iC(\tau)]J_{K+1}(\tilde{U}_pC(\tau))-\{(1+\epsilon^2)B(\tau)\\ +[\epsilon^2D(\tau)-iC(\tau)]e^{i\tau}\}J_K(\tilde{U}_pC(\tau))],\end{aligned} \tag{21}$$

with

$$\tilde{U}_p=U_p\frac{1-\epsilon^2}{1+\epsilon^2}, \tag{22}$$

and $J_K(\cdot)$ denoting the Bessel function of Kth order. The explicit expressions for the functions $B(\tau)$, $C(\tau)$, $D(\tau)$, and $F_K(\tau)$ are given in Appendix B.

B. Numerical results

In the numerical calculations, we calculate the integrals (18) and (19) over a range of typically 4–5 optical cycles. The sum over M is extended to $|M|\simeq 7-8$ in order to get a good convergence (note that the restriction of the sum over M to $M=0$ is equivalent to an appropriately normalized GBR model). Our results for neon are presented in Figs. 1–3. Throughout the paper, we use laser parameters that correspond to the laser used in the experiments of Ref. [14], which produced 150 fs [full width at half maximum (FWHM)] pulses at the wavelength of 825 nm. In our system of units, $I_p=14.4$ and $T_D\simeq 100$.

In Figs. 1 and 2, we present typical results for the intensity dependence of the x and y components of the induced atomic dipole at the 43rd harmonic, for three values of the ellipticity. Figure 2 contains only two curves, since for $\epsilon=0$, the y component of the dipole is zero. The intensity dependences of both $|x_{43}|^2$[Fig. 1(a)], and $|y_{43}|^2$[Fig. 2(a)] show the characteristic transition from the cutoff region (where the dipole strengths increase rapidly) to the plateau region (where the dipole strengths saturate and are dominated by quantum interference effects). With increasing ellipticity, the dipole strength decreases whereas the cutoff position shifts slightly toward higher intensities (hence, for a given intensity, towards lower harmonic orders). In Figs. 1(b) and 2(b), we show the intensity dependences of the phase of the dipole. This phase, as we stressed in Refs. [11,12], determines, to a great extent, the coherence properties of the propagated signal and can be interpreted in quasiclassical terms. It exhibits a piecewise linear behavior as a function of the laser intensity. The slope of the phase for intensities below the cutoff-plateau transition point is equal

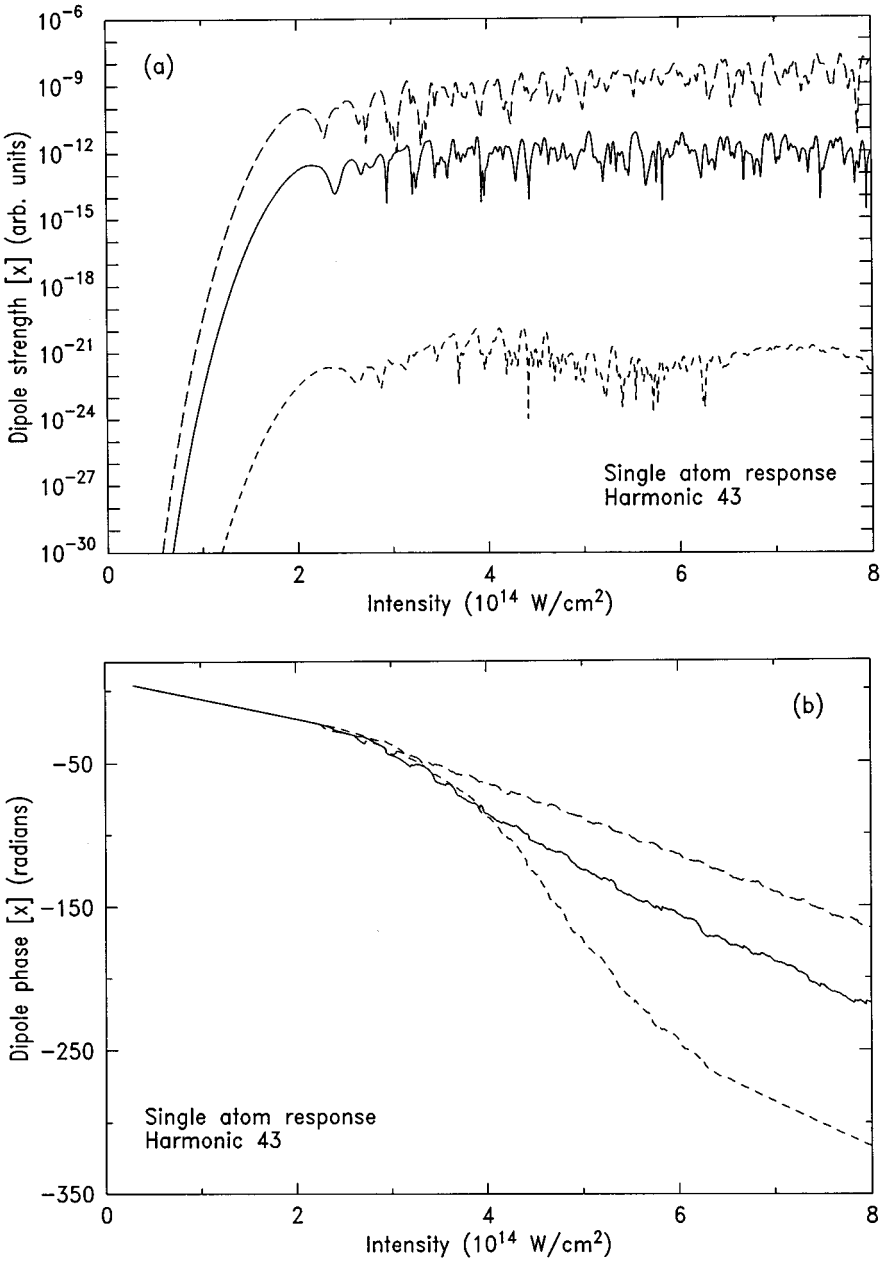

FIG. 1. Strength (a) and phase (b) of the x component of the neon dipole at the 43rd harmonic frequency as a function of the laser intensity, for three values of the ellipticity: $\epsilon=0$ (long-dashed line), $\epsilon=0.3$ (solid line), and $\epsilon=0.6$ (short-dashed line).

to $\simeq -3.2$ in units of U_p. In this regime, it practically does not change with ellipticity. In the plateau region, the phase exhibits oscillations due to quantum interferences. The average slope is larger ($\simeq -5.8$ for $\epsilon=0$) than in the cutoff, and increases with ellipticity ($\simeq -20$ for $\epsilon=0.6$). This increase of the slope with the laser ellipticity takes place over a limited range of intensities [from ~ 2.7 to 6×10^{14} W/cm^2 in Figs. 1(b) and 2(b)]. It strongly depends on the process order, being more and more pronounced as the harmonic order increases (it is very significant for the 63rd harmonic).

As we have shown in Ref. [12], the slope is related to the return time of the electron for the most relevant saddle points. The large slopes obtained for large ellipticities seem to imply that the trajectories corresponding to long return times (i.e., longer than one period with, possibly, multiple returns) play a dominant role in this case, especially for high harmonic orders. Numerical analysis confirms this interpretation. The contributions from high values of the return times are usually cut off due to diffusion effects (which our theory accounts for), and due to electron rescattering effects (which our theory ignores). One could argue that the physical significance of such trajectories could be questioned at small ellipticities, since electron rescattering would eliminate them (see discussion in [9]). At high ellipticities, however, this argument fails, since the effects of rescattering are much weaker, and can be perfectly neglected. These contributions then have to be taken into account, and only quantum diffusion might eliminate them. This effect influences the propagation effects significantly, as we shall see below.

In Fig. 3, we plot the relative harmonic strengths as a function of the laser ellipticity for the (a) 23rd, (b) 43rd, and (c) 63rd harmonics, and for different values of the laser in-

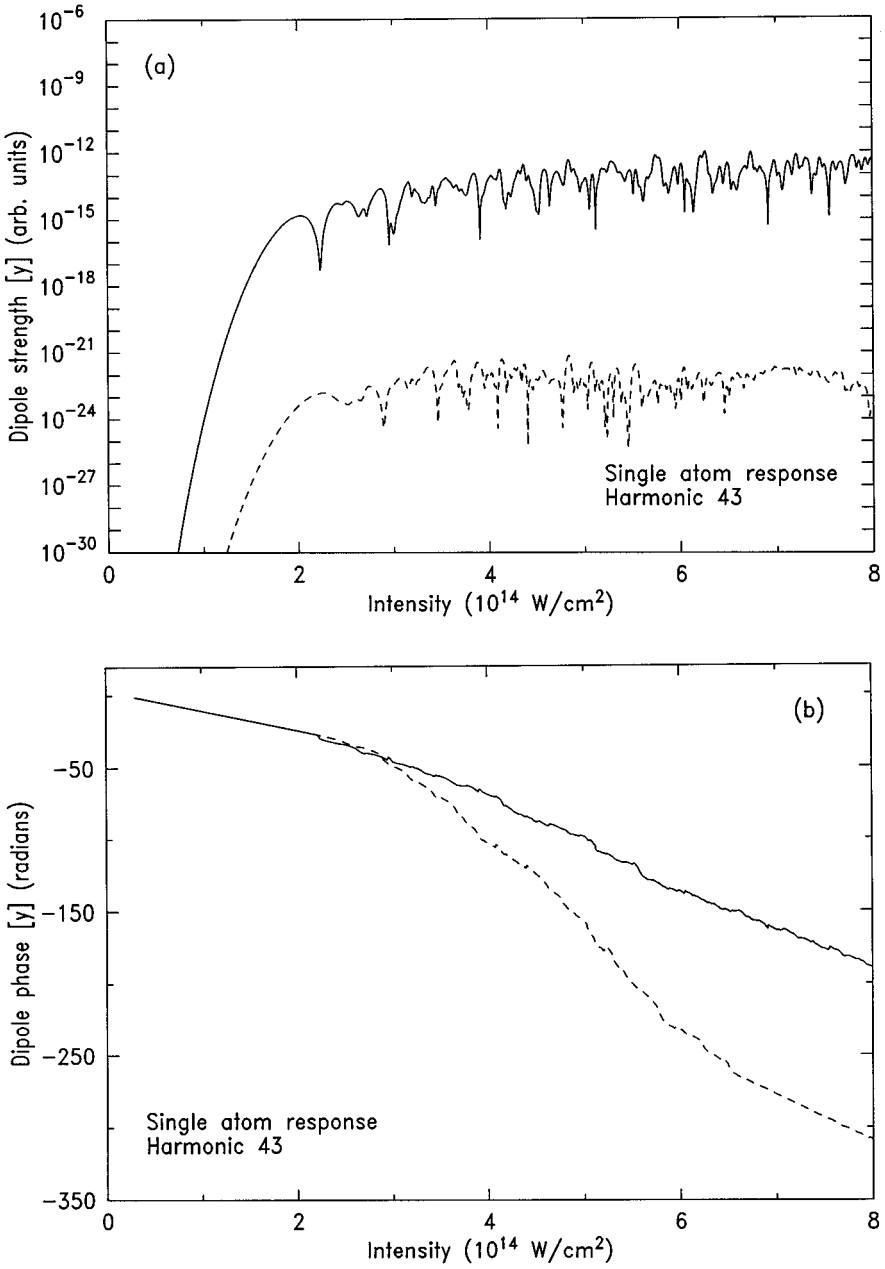

FIG. 2. Strength (a) and phase (b) of the y component of the neon dipole at the 43rd harmonic frequency as a function of the laser intensity, for two values of the ellipticity: $\epsilon = 0.3$ (solid line) and $\epsilon = 0.6$ (short-dashed line).

tensity. The curves are normalized such that the harmonic strengths for $\epsilon = 0$ are set equal to one. The dipole strength decreases drastically (six orders of magnitude at least) as the laser ellipticity increases from 0 (linear polarization) to 0.5 (an ellipticity of 1 corresponds to circular polarization). This effect is more pronounced for high harmonic orders, in agreement with the experimental observations [14,28]. The influence of the laser intensity is not very important. It changes the relative dipole strengths by at most two orders of magnitude, and in a nonmonotonic way [see, for example, Fig. 3(a)]. Interference effects are clearly observed as oscillatory features in Figs. 3(b) and 3(c). They even induce a local minimum at $\epsilon = 0$ at high intensity [see Fig. 3(c)]. Note that this minimum cannot be interpreted in terms of the effects discussed in [17], which apply to much lower harmonic orders (comparable to I_p). It is also worth stressing that the interference effects are smaller in the hydrogen model than in the cruder GBR description. The contributions of several Fourier components of the atomic dipole moments [see Eq. (17)] apparently tend to smooth out quantum interference effects.

The results presented in Fig. 3 have been obtained without taking depletion into account. The effect of depletion is indeed hardly visible on these curves, at the intensities considered ($\leqslant 6 \times 10^{14}$ W/cm^2). The relative harmonic strengths depend on the depletion rate only through the normalization constant N. Since the depletion rate is a weakly decreasing function of the ellipticity, the norm N increases with ellipticity. It thus promotes the regions of large values of ϵ relative to the region $\epsilon \simeq 0$. The resulting broadening of the curves is,

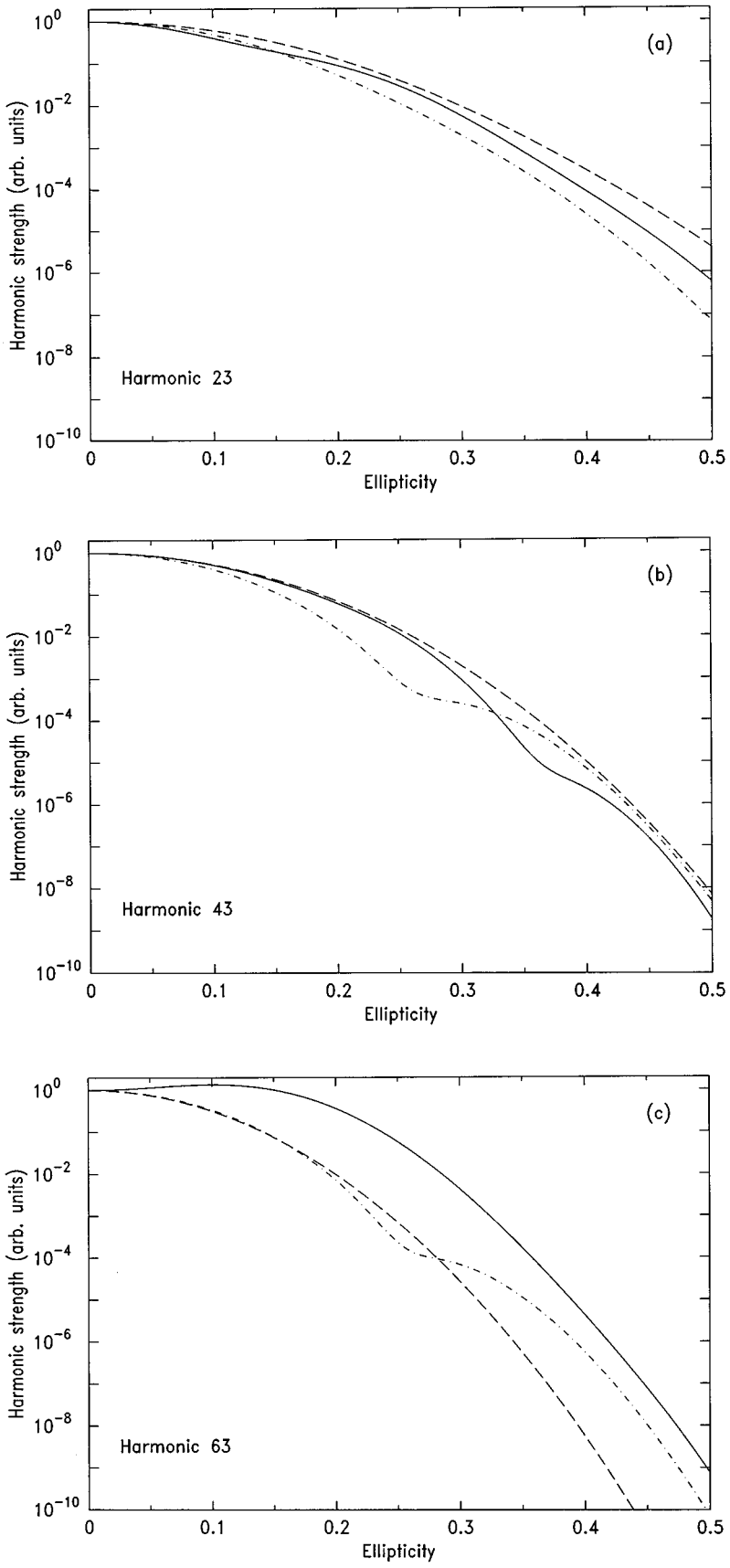

FIG. 3. Relative single-atom harmonic strengths as a function of the laser ellipticity for (a) 23rd, (b) 43rd, and (c) 63rd harmonic, and for three values of the laser intensity: 2×10^{14} W/cm^2 (long-dashed line), 4×10^{14} W/cm^2 (dot-dashed line), and 6×10^{14} W/cm^2 (solid line).

however, visible only at sufficiently high intensities ($\simeq 8\times 10^{14}$ W/cm^2), when the depletion starts playing a significant role. In the following, we shall thus neglect the depletion, keeping in mind what its (small) effect might be. Note that, if we had plotted the absolute harmonic strengths, the effect of depletion would have been more pronounced, since the results for high intensities (high depletion) would have been shifted down along the vertical axis (i.e., reduced in value), by up to one order of magnitude.

III. MACROSCOPIC RESPONSE

The second step of the theoretical description consists of solving the propagation equations in the paraxial and slowly varying envelope approximations, using the dipole moments discussed previously as source terms. The method for solving the propagation equations has been discussed previously for linearly polarized fundamental (and harmonic) fields [23]. In the present paper, we discuss the validity of the different approximations used and we generalize the method to elliptically polarized fields.

A. Propagation equations in homogeneous media

We start from the general wave equation describing the propagation of an electromagnetic field $\vec{\mathscr{E}}(\vec{r},t)$ in an isotropic, globally neutral, nonmagnetic, dielectric medium, characterized by an electronic polarization $\vec{\mathscr{P}}(\vec{r},t)$:

$$\nabla^2\vec{\mathscr{E}}(\vec{r},t)-\frac{1}{c^2}\frac{\partial^2\vec{\mathscr{E}}(\vec{r},t)}{\partial t^2}=\frac{1}{\epsilon_0 c^2}\frac{\partial^2\vec{\mathscr{P}}(\vec{r},t)}{\partial t^2}. \tag{23}$$

It is natural to decompose $\vec{\mathscr{E}}(\vec{r},t)$ and $\vec{\mathscr{P}}(\vec{r},t)$ as sum of harmonic fields and polarizations:

$$\vec{\mathscr{E}}(\vec{r},t)=\sum_q \vec{\mathscr{E}}_q(\vec{r},t);\vec{\mathscr{P}}(\vec{r},t)=\sum_q \vec{\mathscr{P}}_q(\vec{r},t). \tag{24}$$

$\vec{\mathscr{P}}_q(\vec{r},t)$ can be expressed as

$$\vec{\mathscr{P}}_q(\vec{r},t)=\vec{\mathscr{P}}_q^L(\vec{r},t)+\vec{\mathscr{P}}_q^{NL}(\vec{r},t) \tag{25}$$

where $\vec{\mathscr{P}}_q^L(\vec{r},t)$ denotes the *linear response* at the (harmonic) frequency and $\vec{\mathscr{P}}_q^{\mathrm{NL}}(\vec{r},t)$ the *nonlinear response*. We assume that the linear response takes the simple form:

$$\vec{\mathscr{P}}_q^L(\vec{r},t)=\epsilon_0\chi_q\vec{\mathscr{E}}_q(\vec{r},t), \tag{26}$$

the susceptibility χ_q being related to the wave vector k_q by $k_q^2=(q\omega/c)^2\epsilon(q\omega)$, with $\epsilon(q\omega)=1+\chi_q$. The refractive index n_q is equal to $\sqrt{\epsilon(q\omega)}$. For the sake of simplicity, we here neglect nonlinear corrections to the linear susceptibility and assume the medium to be homogeneous. We will come back on these points in the next section. The nonlinear response of the medium, $\vec{\mathscr{P}}_q^{\mathrm{NL}}(\vec{r},t)$, includes, in principle, contributions from a large number of processes involving the harmonic and fundamental fields. We neglect the influence of wave mixing processes involving harmonic fields as well as the depletion of the fundamental field by energy transfer to the harmonic fields. Both assumptions are justified owing to the relatively low conversion efficiency for these high-order processes. $\vec{\mathscr{P}}_q^{\mathrm{NL}}$ is therefore the polarization induced by the fundamental field only. Introducing the electric excitation $\vec{\mathscr{D}}_q=\epsilon_0\vec{\mathscr{E}}_q+\vec{\mathscr{P}}_q^L$, Eq. (23) becomes a set of equations:

$$\nabla^2\vec{\mathscr{E}}_1(\vec{r},t)-\frac{1}{\epsilon_0 c^2}\frac{\partial^2\vec{\mathscr{D}}_1(\vec{r},t)}{\partial t^2}=\vec{0},$$

$$\nabla^2\vec{\mathscr{E}}_q(\vec{r},t)-\frac{1}{\epsilon_0 c^2}\frac{\partial^2\vec{\mathscr{D}}_q(\vec{r},t)}{\partial t^2}=\frac{1}{\epsilon_0 c^2}\frac{\partial^2\vec{\mathscr{P}}_q^{\mathrm{NL}}(\vec{r},t)}{\partial t^2}. \tag{27}$$

These equations are only coupled through the dependence of $\vec{\mathscr{P}}_q^{\mathrm{NL}}(\vec{r},t)$ on $\vec{\mathscr{E}}_1(\vec{r}',t')$ (it may not be a local function of the electric field). Note that, at this point, we have not made any paraxial or slowly varying envelope approximations. We now introduce the envelope functions $\vec{E}_q$ and $\vec{P}_q^{\mathrm{NL}}$

$$\vec{\mathscr{E}}_q(\vec{r},t)=\frac{1}{2}\vec{E}_q(\vec{r},t)e^{i(k_q z-q\omega t)}+\text{ c.c.},$$

$$\vec{\mathscr{P}}_q^{\mathrm{NL}}(\vec{r},t)=\frac{1}{2}\vec{P}_q^{\mathrm{NL}}(\vec{r},t)e^{i(qk_1 z-q\omega t)}+\text{ c.c.} \tag{28}$$

ω is the laser frequency and z denotes the coordinate on the propagation axis. In the paraxial approximation, the field $\vec{\mathscr{E}}(\vec{r},t)$ and the polarization $\vec{\mathscr{P}}(\vec{r},t)$ are supposed to be perpendicular to the propagation axis z, i.e., in the (x, y) plane. Further, we make the slowly varying envelope approximation, i.e., we assume that $\vec{E}_q(\vec{r},t)$, $\vec{P}_q^{\mathrm{NL}}(\vec{r},t)$ vary slowly in time over the *harmonic* period and in the coordinate z over the harmonic wavelength. Although for short laser pulses and high intensities, the nonlinear polarization may vary rapidly in time, compared to the exciting *laser* period, we believe that the slowly varying envelope approximation is satisfied for the harmonic propagation equations. After a few manipulations described in textbooks (see, e.g. [29]), Eq. (27) becomes

$$\nabla_\perp^2\vec{E}_1(\vec{r},t)+2ik_1\left(\frac{\partial\vec{E}_1(\vec{r},t)}{\partial z}+\frac{1}{v_{g1}}\frac{\partial\vec{E}_1(\vec{r},t)}{\partial t}\right)=\vec{0},$$

$$\nabla_\perp^2\vec{E}_q(\vec{r},t)+2ik_q\left(\frac{\partial\vec{E}_q(\vec{r},t)}{\partial z}+\frac{1}{v_{gq}}\frac{\partial\vec{E}_q(\vec{r},t)}{\partial t}\right)$$
$$=-\frac{q^2\omega^2}{\epsilon_0 c^2}\vec{P}_q^{\mathrm{NL}}(\vec{r},t)\exp(-i\Delta k_q z). \tag{29}$$

v_{gq} denotes the group velocity at frequency $q\omega$ and $\Delta k_q=k_q-qk_1$, the phase mismatch. $\nabla_\perp^2$ is the Laplacian operating on the transverse coordinates (x, y), or when the problem is axisymmetric, on the coordinate r. To obtain Eq. (29), we have neglected the double derivatives of $\vec{E}_q(\vec{r},t)$ relative to z and t and we have assumed $\partial^2\vec{\mathscr{P}}_q(\vec{r},t)/\partial t^2\simeq -q^2\omega^2\vec{\mathscr{P}}_q(\vec{r},t)$. Assuming equal group velocities for all the frequencies (which is valid for the small and diluted media considered in the high-order harmonic generation experiments) and making the change of variables

$\vec{r'}=\vec{r};t'=t-z/v_g$, which amounts to using the referential moving at the common group velocity, we obtain

$$\nabla_\perp^2\vec{E}_1(\vec{r'},t')+2ik_1\frac{\partial\vec{E}_1(\vec{r'},t')}{\partial z'}=\vec{0},$$

$$\nabla_\perp^2\vec{E}_q(\vec{r'},t')+2ik_q\frac{\partial\vec{E}_q(\vec{r'},t')}{\partial z'}=-\frac{q^2\omega^2}{\epsilon_0c^2}\vec{P}_q^{\rm NL}(\vec{r'},t')e^{-i\Delta k_qz'} \quad (30)$$

(we drop the primes from now on). So far, we have not specified the dependence of the polarization on the incident field. We now assume that the polarization is a *local* function of the incident electric field, both in space and time. The field creating a polarization in $(\vec{r},t)$ is $\vec{\mathscr{E}}_1(\vec{r},t)$. In space, this approximation is valid for the dilute media used in the present problem. In time, the implication that the polarization follows "instantaneously" the change in electric field, might be questionable for high intensities and short pulses. The validity of the temporal locality will be investigated in future work. Here, we simply approximate the nonlinear polarization, in the framework of the dipole approximation, by

$$\vec{P}_q^{\rm NL}(\vec{r},t)=2\mathscr{N}\vec{x}_q(\vec{r},t)e^{iq\phi_1(\vec{r},t)}, \quad (31)$$

where $\mathscr{N}$ is the atomic density, and $\vec{x}_q(\vec{r},t)$, the harmonic component of the atomic dipole moment, calculated for a field $[|E_{1x}|\cos(\omega t),|E_{1y}|\sin(\omega t),0]$. The factor of 2 arises from different conventions used in the definitions of $\vec{P}_q^{\rm NL}$[Eq. (28)] and $\vec{x}_q$[Eq. (5)]. Finally, $\phi_1(\vec{r},t)$ represents the phase of the laser field envelope $\vec{E}_1(\vec{r},t)$, obtained by solving the propagation equation for the fundamental.

B. Propagation equations in inhomogeneous media

The propagation equations [Eq. (30)] are immediately generalized to the case of neutral media, with a z-dependent atomic density, $\mathscr{N}(z)$. In Eqs. (28), (29), and (30), k_1z, k_qz, and Δk_qz are replaced by $\int^z k_1(z')dz'$, $\int^z k_q(z')dz'$, and $\int^z\Delta k_q(z')dz'$, respectively.

When the medium is *absorbing* at frequency $q\omega$, $|\vec{E}_q(\vec{r},t)|=|\vec{\mathscr{E}}_q(\vec{r},t)|\exp[\int^z\kappa_q(z')dz']$, where κ_q is the absorption coefficient at frequency $q\omega$ (imaginary part of k_q). It is then more convenient to introduce a new envelope function for the harmonic fields $\tilde{\vec{E}}_q(\vec{r},t)=\vec{E}_q(\vec{r},t)\exp[i\int^z\Delta k_q(z')dz']$, such that $|\tilde{\vec{E}}_q(\vec{r},t)|=|\vec{\mathscr{E}}_q(\vec{r},t)|$. The propagation equations (30) become

$$\nabla_\perp^2\vec{E}_1(\vec{r},t)+2ik_1\frac{\partial\vec{E}_1(\vec{r},t)}{\partial z}=\vec{0},$$

$$\nabla_\perp^2\tilde{\vec{E}}_q(\vec{r},t)+2ik_q\frac{\partial\tilde{\vec{E}}_q(\vec{r},t)}{\partial z}+2k_q\Delta k_q(z)\tilde{\vec{E}}_q(\vec{r},t)=-\frac{q^2\omega^2}{\epsilon_0c^2}\vec{P}_q^{\rm NL}(\vec{r},t). \quad (32)$$

The case of inhomogeneous media owing to (partial) ionization is more difficult and requires additional approximations. The refractive index n_q contains contributions from atoms, ions (which we assume, for simplicity, to be only singly charged), and electrons,

$$[n_q(\vec{r},t)]^2=1+\chi_q^a(\vec{r},t)+\chi_q^i(\vec{r},t)+\chi_q^e(\vec{r},t), \quad (33)$$

where the indices a,i, and e refer to the atomic, ionic, and electronic susceptibilities, respectively. $\chi_q^{a,i}(\vec{r},t)=\mathscr{N}^{a,i}(\vec{r},t)\alpha^{a,i}(q\omega)$, where $\alpha^{a,i}(q\omega)$ and $\mathscr{N}^{a,i}(\vec{r},t)$ denote the (atomic or ionic) dipole polarizability and density. We do not consider here nonlinear corrections to the polarizabilities. In the calculations presented below, we shall actually completely neglect the atomic and ionic dispersion, considering only the dispersion induced by the electrons. The electronic term takes a simple form:

$$\chi_q^e(\vec{r},t)=-\frac{e^2\mathscr{N}^e(\vec{r},t)}{mq^2\omega^2}. \quad (34)$$

For short laser pulses, the electrons do not have time to move so that the electronic density $\mathscr{N}^e(\vec{r},t)\simeq\mathscr{N}^i(\vec{r},t)$. This approximation allows us to keep the cylindrical symmetry relative to the propagation axis. We express the refractive index and the wave vector as

$$[n_q(\vec{r},t)]^2=1+\chi_q^0(z)+\delta\chi_q(\vec{r},t),$$

$$k_q(\vec{r},t)=n_q(\vec{r},t)q\omega/c=k_q^0(z)+\delta k_q(\vec{r},t), \quad (35)$$

with $\chi_q^0(z)=\mathscr{N}(z)\alpha^a(q\omega)$, $\mathscr{N}(z)$ being the (initial) medium density, and $k_q^0(z)=(q\omega/c)[1+\chi_q^0(z)/2]$. We have here extracted the contributions from the atomic medium, assumed to be not depleted by ionization $[1+\chi_q^0(z)$ and $k_q^0(z)]$. The remaining contributions to the refractive index and the wave vector induced by ionization are written as correction terms $\delta\chi_q(\vec{r},t)$ and $\delta k_q(\vec{r},t)$, respectively. Note that we could also, more simply, consider the wave vector describing propagation in vacuum: $k_q^0=q\omega/c$, including all dispersion effects in δk_q.

The linear response of the medium [see Eq. (26)] can be written as

$$\vec{\mathscr{P}}_q^L(\vec{r},t)=\epsilon_0\chi_q^0(z)\vec{\mathscr{E}}_q(\vec{r},t)+\epsilon_0\delta\chi_q(\vec{r},t)\vec{\mathscr{E}}_q(\vec{r},t). \quad (36)$$

The first term in the sum is treated as before by moving it to the left-hand side of the propagation equation, incorporating it by means of the wave vector k_q^0. The second term is considered as an additional source term to the propagation equations, to which the slowly varying envelope approximation can be applied, i.e., $\partial^2\delta\chi_q(\vec{r},t)\vec{\mathscr{E}}_q(\vec{r},t)/\partial t^2\simeq-q^2\omega^2\delta\chi_q(\vec{r},t)\vec{\mathscr{E}}_q(\vec{r},t)$. Following the derivation of the preceding section, and using the envelopes defined by

$$\vec{\mathscr{E}}_q(\vec{r},t)=\frac{1}{2}\vec{E}_q(\vec{r},t)e^{i[q\int^z k_q^0(z')dz'-q\omega t]}+\text{c.c.}$$

$$\vec{\mathscr{P}}_q^{\rm NL}(\vec{r},t)=\frac{1}{2}\vec{P}_q^{\rm NL}(\vec{r},t)e^{i[q\int^z k_1^0(z')dz'-q\omega t]}+\text{c.c.}, \quad (37)$$

Eq. (32) becomes

$$\nabla_\perp^2\vec{E}_1(\vec{r},t)+2ik_1^0\frac{\partial\vec{E}_1(\vec{r},t)}{\partial z}+2k_1^0\delta k_1(\vec{r},t)\vec{E}_1(\vec{r},t)=\vec{0}, \quad (38)$$

$$\nabla_\perp^2\vec{E}_q(\vec{r},t)+2ik_q^0\frac{\partial\vec{E}_q(\vec{r},t)}{\partial z}+2k_q^0[\Delta k_q^0(z)+\delta k_q(\vec{r},t)]\vec{E}_q(\vec{r},t)=-\frac{q^2\omega^2}{\epsilon_0c^2}\vec{P}_q^{\rm NL}(\vec{r},t). \quad (39)$$

C. Numerical results

The propagation equations [Eqs. (38) and (39)] are solved numerically over the length of the nonlinear medium using a finite-difference technique. They are discretized in the (r,z) plane on a 500×300 point grid and integrated using a space-marching Crank-Nicholson scheme. The field at the position z_i is obtained from that at the position z_{i-1} by inverting a tridiagonal matrix with a classical recursive algorithm. Equation (38), nonlinear through the dependence of $\delta k_1(\vec{r},t)$ on the field intensity is solved first, for the two components of the (elliptically polarized) incident field. Next, one calculates $\vec{P}_q^{\rm NL}(\vec{r},t)$ and $\delta k_q(r,z)$ induced by the *perturbed* fundamental field $\vec{E}_1(\vec{r},t)$. Then, Eq. (39) is solved, yielding the harmonic field $\vec{E}_q(\vec{r},t)$. This is repeated for a sequence of times t spanning the laser pulse duration (typically 30 points). To obtain the harmonic strengths, we integrate $|\vec{E}_q(\vec{r},t)|^2$ at the exit of the medium, over the transverse coordinate r (using cylindrical coordinates), and over the laser pulse duration. As in Sec. II, we use parameters close to the experimental conditions of [14]. The laser is assumed to be Gaussian in space and time, with a 5-mm confocal parameter and a 150-fs pulse duration at half maximum. The atomic density profile is a truncated Lorentzian function with a 0.8-mm FWHM, centered at the laser focus. This is not the best condition for generating coherent harmonics [11,12], but no optimization with respect to the focus position has been done in the experiments. The peak density is taken to be 15 Torr. The dimension of the grid in space is approximately (depending on the process order) 100 μm $\times$1.6 mm, and in time, 250 fs.

For low laser frequencies, pressures above 10 Torr and intensities high enough to partially ionize the medium, the refractive index will be dominated by the free electron contribution. In the calculations presented below, we neglect all atomic or ionic dispersion effects, as well as absorption, but we include the effects of depletion and the dispersion induced by free electrons. In Eqs. (38) and (39), we set $k_q^0=q\omega/c$, $\Delta k_q^0(z)=0$, and $\delta k_q(\vec{r},t)=-e^2\mathscr{N}^e(\vec{r},t)/2mqc\omega$. The electronic density is obtained from the tunneling ionization rates $\Gamma(|\vec{E}_1|)$ derived in Sec. II as

$$\mathscr{N}^e(\vec{r},t)=\mathscr{N}(z)\left[1-\exp\left(-\int_{-\infty}^{t}\Gamma[|\vec{E}_1(\vec{r},t')|]dt'\right)\right]. \quad (40)$$

The dispersion introduced by the free electrons has several effects: it introduces an additional phase mismatch, thus deteriorating phase matching. It leads to defocusing and blue-shifting of the fundamental field. These effects play a dominant role in some situations [30]. For the intensities and density used in these calculations, however, they remain marginal. We checked that they do not influence the polarization properties of the generated harmonic field in any significant way.

In Fig. 4, we compare the single-atom results (solid line) with the propagated signals (dashed line) for the (a) 23rd, (b) 43rd, and (c) 63rd harmonics at an intensity of 6×10^{14} W/cm^2. For the calculation including propagation, this intensity is to be understood as the peak intensity. The first conclusion to be drawn from the figure is that propagation (and time-averaging) smooths out quantum interference patterns. In general, the propagated results decrease faster with ellipticity than in the single-atom response, especially for high-order harmonics [see Fig. 4(c)]. The result in Fig. 4(b), which is at variance with this tendency, is probably due to the destructive interfence effect occurring at $\epsilon\simeq0.35$, which reduces, in this case, the single-atom response. The faster decrease with ellipticity in the propagated results can be explained by the previously noted increase of the variation of the phase in the plateau region with the laser ellipticity [see Figs. 1 and 2(b)], which deteriorates phase matching for large ellipticities.

In Fig. 5, we compare the results of our calculation (including propagation) with experimental data for the (a) 23rd, (b) 43rd, (c) 63rd harmonics. In each plot, we present three theoretical curves corresponding to the laser peak intensities 2, 4, and 6×10^{14} W/cm^2 [only the last two are shown in Fig. 5(c), the 63rd-harmonic generation efficiency at 2×10^{14} W/cm^2 being negligible]. The full circles denote the result of the experiment performed by Budil *et al.* [14]. The open squares are the results of recent experiments carried out at Saclay with a Ti:sapphire laser at a slightly different wavelength, 790 nm, but otherwise in very similar conditions [28]. This laser has a higher repetition rate (20 Hz) than the one used in [14], thus allowing for better statistics. The agreement between theory and experiment is very good, irrespective of the laser intensity used in the calculations (which does not influence much the results). In particular, the theory reproduces extremely well the significant narrowing of the ellipticity dependence with increasing harmonic number [compare Figs. 5(a) and 5(c)]. The deviation observed at large ellipticities is simply due to the fact that, in the experiments, the signal was barely above the noise level, and measured with poor accuracy in this region.

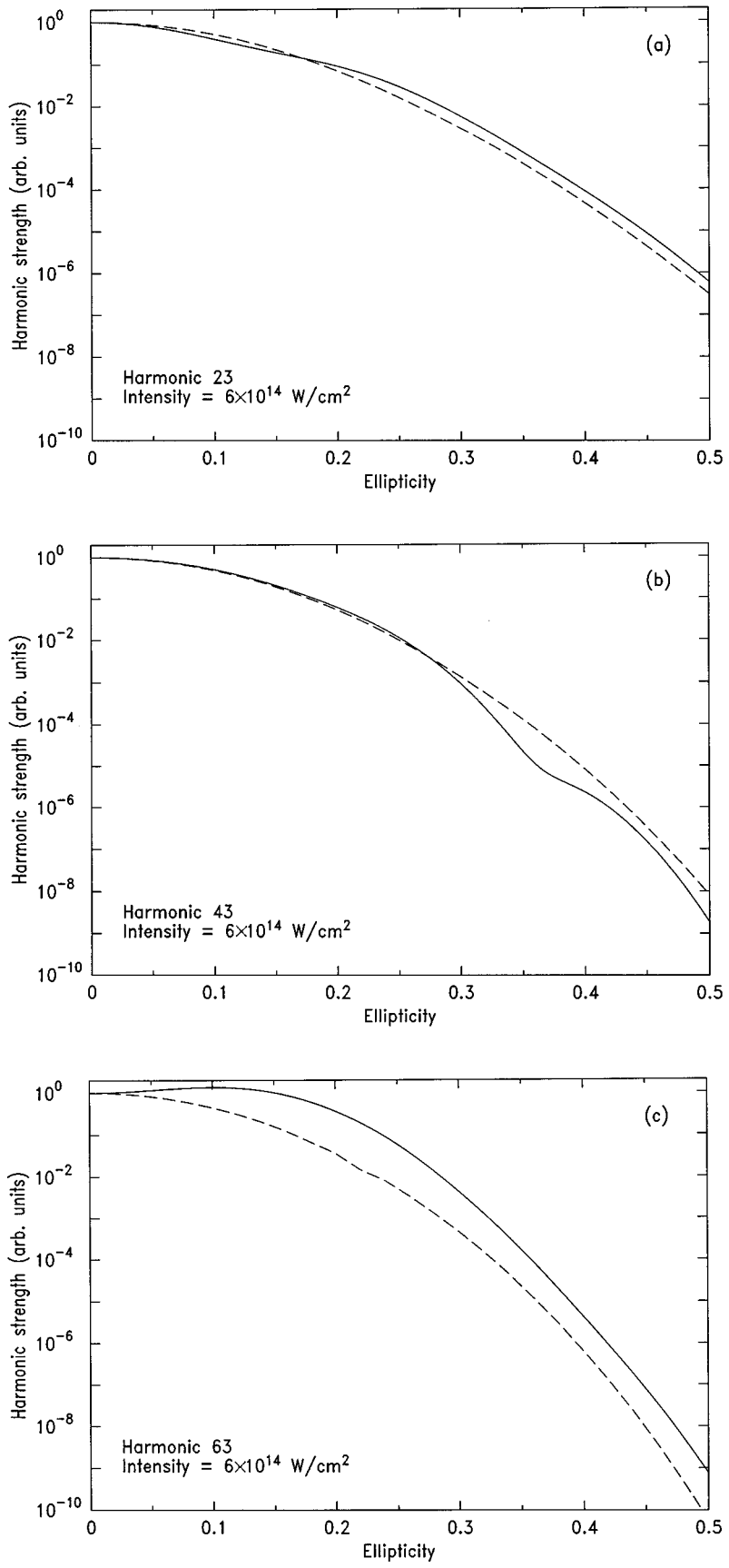

FIG. 4. Comparison of the single-atom (solid line) and propagated (dashed line) harmonic strengths for (a) 23rd, (b) 43rd, and (c) 63rd harmonic, at a peak laser intensity of 6×10^{14} W/cm^2.

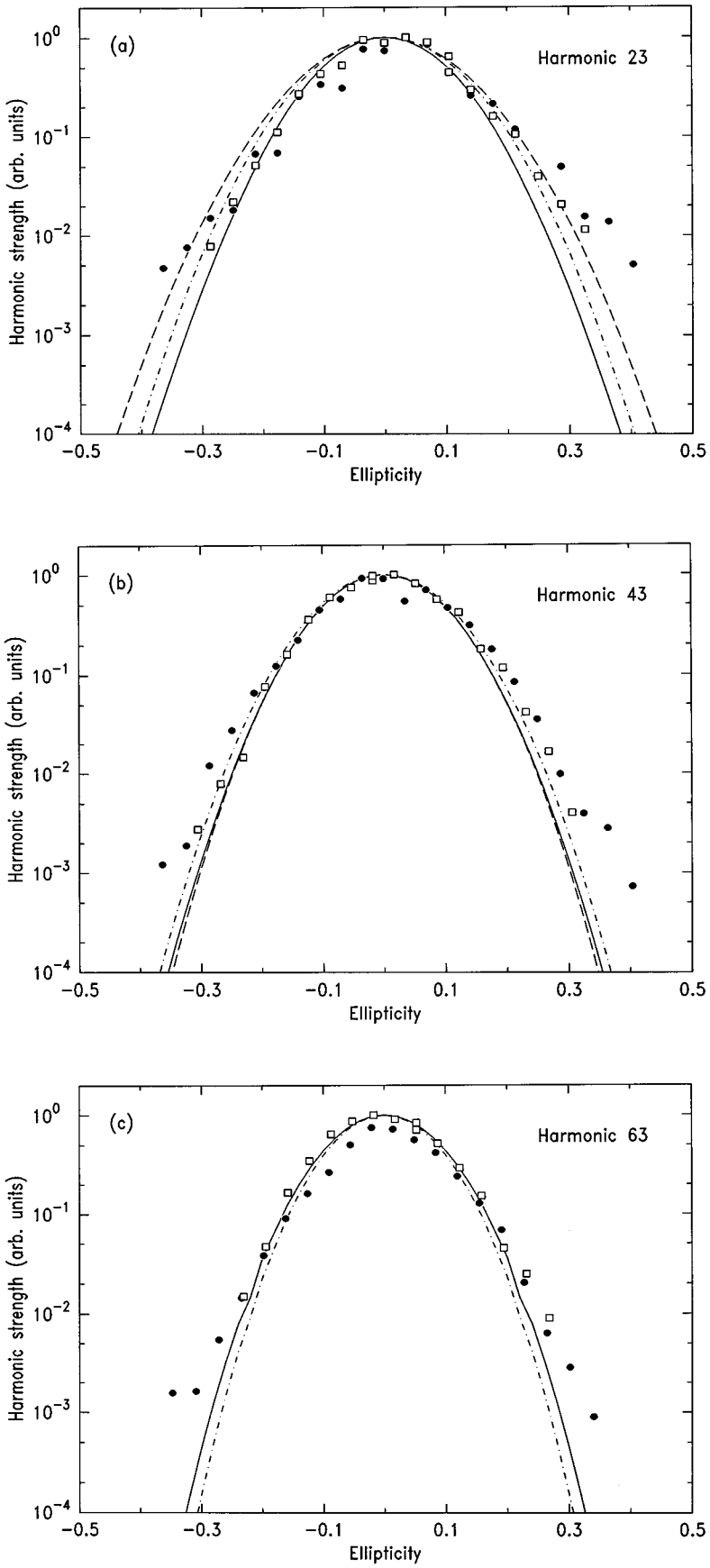

FIG. 5. Comparison of the simulated harmonic strengths with experimental data for (a) 23rd, (b) 43rd, and (c) 63rd harmonic. Theoretical curves correspond to three different peak intensities: 2×10^{14} W/cm^2 (long-dashed line), 4×10^{14} W/cm^2 (dot-dashed line), and 6×10^{14} W/cm^2 (solid line). Only the last two intensities are plotted for the 63rd harmonic since it is very far in the cutoff region at low intensity. Full circles denote experimental data from Ref. [14]. Open squares denote recent results obtained at Saclay with a Ti:S laser [28].

IV. POLARIZATION OF HARMONICS

Before presenting numerical results, we discuss how to extract from the calculated dipole component $\vec{x}_q$ in the single-atom response, and from the complex space- and time-dependent harmonic field $\vec{E}_q(\vec{r},t)$ in the macroscopic response, the polarization of the harmonics. We use the Stokes parameters, following Born and Wolf [31].

A. Stokes parameters

For an elliptically polarized light field ($E_x e^{-i\phi_x}$, $E_y e^{-i\phi_y}$, 0), the Stokes parameters s_0, s_1, s_2, and s_3 are defined by

$$s_0 = E_x^2 + E_y^2 \ \text{(intensity)},$$

$$s_1 = E_x^2 - E_y^2,$$

$$s_2 = 2E_x E_y \cos(\phi) \ \text{, with } \phi = \phi_y - \phi_x,$$

$$s_3 = 2E_x E_y \sin(\phi). \tag{41}$$

Note that $s_0^2 = s_1^2 + s_2^2 + s_3^2$. Let ψ be the angle of rotation of the major axes of the ellipse in the (x,y) plane (defined with respect to the x axis) and χ the parameter characterizing, at the same time, the ellipticity of the field and the sense of rotation of the ellipse (*helicity*); more precisely, let $\tan(\chi) = \pm b/a$, b and a denoting, correspondingly, the minor and major axes of the ellipse, and b/a denoting the ellipticity. The sign is positive for right-handed polarization, i.e., such that, to an observer looking in the direction from which the light is coming, the electric field vector turns in the clockwise sense. χ and ψ are related to the Stokes parameters by the relations:

$$s_1 = s_0 \cos(2\chi)\cos(2\psi),$$

$$s_2 = s_0 \cos(2\chi)\sin(2\psi),$$

$$s_3 = s_0 \sin(2\chi),$$

$$s_2 = s_1 \tan(2\psi). \tag{42}$$

Equations (41) and (42) allow us to calculate simply the polarization properties of the harmonics in the single-atom response.

The interest of the Stokes parameters is that they can also be defined as results of simple experiments consisting in measuring the intensity of the light passing through a combination of polarizer and compensator. Let us introduce $I(\theta,\varphi)$ as the intensity of light vibration in the direction making an angle θ with the x axis, when the y component is subjected to a retardation φ with respect to the x component. The Stokes parameters can be expressed as

$$s_0 = I(0,0) + I(\pi/2,0),$$

$$s_1 = I(0,0) - I(\pi/2,0),$$

$$s_2 = I(\pi/4,0) - I(3\pi/4,0),$$

$$s_3 = I(\pi/4,\pi/2) - I(3\pi/4,\pi/2). \tag{43}$$

These definitions (43) do not require the light source to be polarized. They can therefore be used to characterize the polarization properties of a *partially* polarized light source, i.e., such that the phase difference ϕ between the two components of the field is not fixed and varies with time and/or space. The *degree of polarization* of a light source is defined by

$$\mathscr{P} = \frac{\sqrt{s_1^2 + s_2^2 + s_3^2}}{s_0}. \tag{44}$$

In general, $\mathscr{P}$ is less than 1, and equal to 1 only for completely polarized radiation. The angle of rotation, and ellipticity (helicity) of an ''average'' ellipse, are defined through the relations:

$$\tan(2\psi) = \frac{s_2}{s_1},$$

$$\sin(2\chi) = \frac{s_3}{\sqrt{s_1^2 + s_2^2 + s_3^2}}. \tag{45}$$

The harmonic radiation generated by high-order conversion of an elliptically polarized laser field, $\vec{E}_q(\vec{r},t)$, is only *partially* polarized, because the phase difference $\phi(\vec{r},t)$ between the x and y components varies, in *space*, over the beam profile, and in *time*, over the pulse duration. We define the polarization properties of the harmonic field with the help of the Stokes parameters [Eq. (43)]. We calculate $I(\theta,\varphi)$ as we would measure it in an experiment:

$$I(\theta,\epsilon) = \int\int |E_{qx}(r,z,t)\cos(\theta) + E_{qy}(r,z,t)\sin(\theta)e^{i\varphi}|^2 2\pi r dr dt. \tag{46}$$

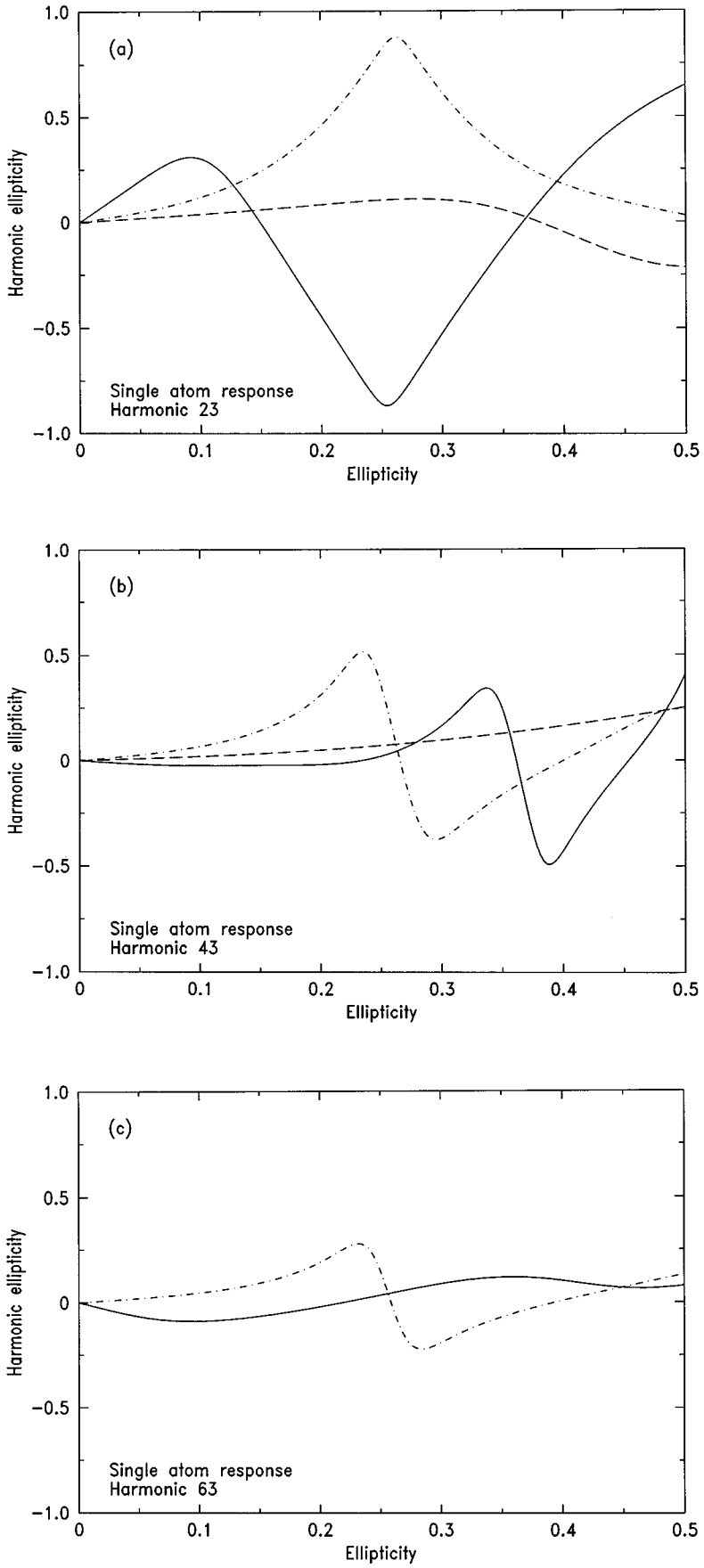

FIG. 6. Ellipticity of the (a) 23rd, (b) 43rd, and (c) 63rd harmonics generated by a single atom as a function of the laser ellipticity, and for three values of the laser intensity: 2×10^{14} W/cm^2 (long-dashed line), 4×10^{14} W/cm^2 (dot-dashed line), and 6×10^{14} W/cm^2 (solid line).

In this equation, E_{qx}, E_{qy} represent the *complex* x and y components of the total field $\vec{E}_q(r,z,t)$. $I(\theta,\varphi)$ is calculated at the exit of the medium (it does not depend on the coordinate z, as long as z is outside the medium). If the degree of polarization $\mathscr{P}=1$, the ellipticity of the field can be determined from s_0, s_1, and s_2 [compare Eqs. (44) and (45)]. It is worth stressing, however, that in general, when $\mathscr{P}<1$, it is necessary to measure s_3 in order to determine the ellipticity of the fields. The experimental determination of the ellipticity is obviously more difficult in this case than the determination of the rotation angle, which can be done by performing contrast measurements (amounting to measuring s_1 and s_2), as explained in Ref. [19].

B. Numerical results

Our results are organized as follows: we present two series of figures, one for the single atom, the other for the macroscopic results, concerning successively the harmonic ellipticity and the rotation angle. Figure 6 shows the variation of the ellipticity of the (a) 23rd, (b) 43rd, (c) 63rd harmonics generated by a single atom, as a function of the laser ellipticity and for different values of laser intensity. At low intensities and small ellipticities (i.e., for harmonics in the cutoff region), the ellipticity of the harmonic is a linear function of the ellipticity of the laser, $\epsilon_{\text{harm}} \propto \epsilon$. The proportionality factor is smaller than one [see the dashed curves in Figs. 6(a) and 6(b)]. At higher intensities (when the harmonics enter the plateau) and higher ellipticities, the ellipticity of the harmonics is a rapidly changing function of the laser ellipticity and exhibits several local maxima and minima [see all other curves in Figs. 6(a)–6(c)]. We attribute these variations to quantum interference effects. Note that the harmonic ellipticity may change sign, which means that the helicity of the harmonic undergoes a dynamically induced jump (this effect is seen practically in all curves in Fig. 6).

Figure 7 presents the same quantities as Fig. 6, but for the macroscopic response. Propagation smooths out the quantum interferences, but only partly, in particular for low-order harmonics [Fig. 7(a)]. Note, that, in contrast to the harmonic strengths (Fig. 5), the results are quite dependent on the laser intensity. The harmonic ellipticity becomes significantly smaller with increasing laser intensity.

In Figs. 8 and 9, we present single-atom and macroscopic results concerning the rotation angle of the harmonic ellipse with respect to the fundamental, as a function of the laser ellipticity. For low process orders, low intensities and low ellipticities, the rotation angle is a linear function of the laser ellipticity, and may reach $20°-30°$ [see the dashed line in Fig. 8(a)]. For high-order harmonics, low intensities and low ellipticities, the rotation of the ellipse is hardly visible [see the dashed line in Fig. 8(b) and the solid line in Fig. 8(c)]. For high intensities and ellipticities, the rotation angle becomes a rapidly varying function of both laser ellipticity and intensity, and exhibits quantum interference effects. The rotation angles for the high-order harmonics [see Figs. 8(b) and 8(c)] are, in general, apart from a narrow ellipticity range, smaller ($\simeq 5°-10°$) than for low-order harmonics [which are close to 60°; see Fig. 8(a)].

Propagation smooths out interference features quite efficiently, as shown in Fig. 9. For low-order harmonics, the rotation angle increases approximately linearly with the laser ellipticity up to about 30°, then saturates. This result is consistent with the experiments of Ref. [19], performed, however, for lower harmonic orders. For the 43rd harmonic, the linear increase of the angle stops at about 7°, and is followed by a decrease. The rotation angles for the high-order harmonics remain practically equal to zero ($<5°$).

In Fig. 10, we show similar results (i.e., same harmonics and intensities) for the polarization degree. Here, we consider only the propagated results, since, for a single atom, the polarization degree is by definition equal to 1. The polarization degree remains close to 1 for high-order process. It deviates from 1 for high intensities, large ellipticities, and low process orders. It remains, however, practically always larger than 0.65.

V. CONCLUSION

In conclusion, we have presented a theoretical approach to harmonic generation by elliptically polarized fields. The single-atom part is a generalization of the theory developed in [8,9]. Numerical calculations are presented for the 23rd, 43rd, and 63rd harmonics of 825-nm-wavelength light. The harmonic strengths decrease rapidly with ellipticity, and exhibit quantum intereferences.

The macroscopic response of the nonlinear medium is calculated within the slowly varying envelope and paraxial approximations. The effect of propagation is to smooth out interference features and to make the decrease of harmonic strength versus ellipticity even faster, especially for the high-order harmonics. This is attributed to the increase of the phase variation of the dipole for large ellipticities, which we interpret as due to the influence of electron trajectories with several returns. The numerical results obtained agree very well with the experimental data.

The polarization properties of the generated light are extracted with the help of the Stokes parameters. The single-atom response is dominated by quantum interference effects and exhibit rapid variations of the ellipticity as well rotation angle as a function of the laser ellipticity, especially for low-order harmonics. Propagation partly smooths out the quantum interference effects. The rotation angle of the ellipse with respect to the fundamental is quite important ($\sim 30°$) for low-order harmonics, in agreement with experiments. Note that the harmonic fields generated in the macroscopic response are only partially polarized. Their degree of polarization remains, however, close to unity.

The theory developed in the present manuscript provides the ground for treating other appealing problems, dealing with the control of harmonics using more sophisticated fundamental fields (with a polarization that varies during the laser pulse [20], or involving several colors). These aspects will be addressed in future work.

ACKNOWLEDGMENTS

We acknowledge fruitful discussions with P. H. Bucksbaum, M. Yu. Ivanov, K. J. Schafer and K. C. Kulander.

APPENDIX A: FOURIER COMPONENTS OF THE FIELD-FREE DIPOLE MOMENT

Here we present a derivation of the analytic expression for the coefficients $b_M(\tau)$. Let us introduce

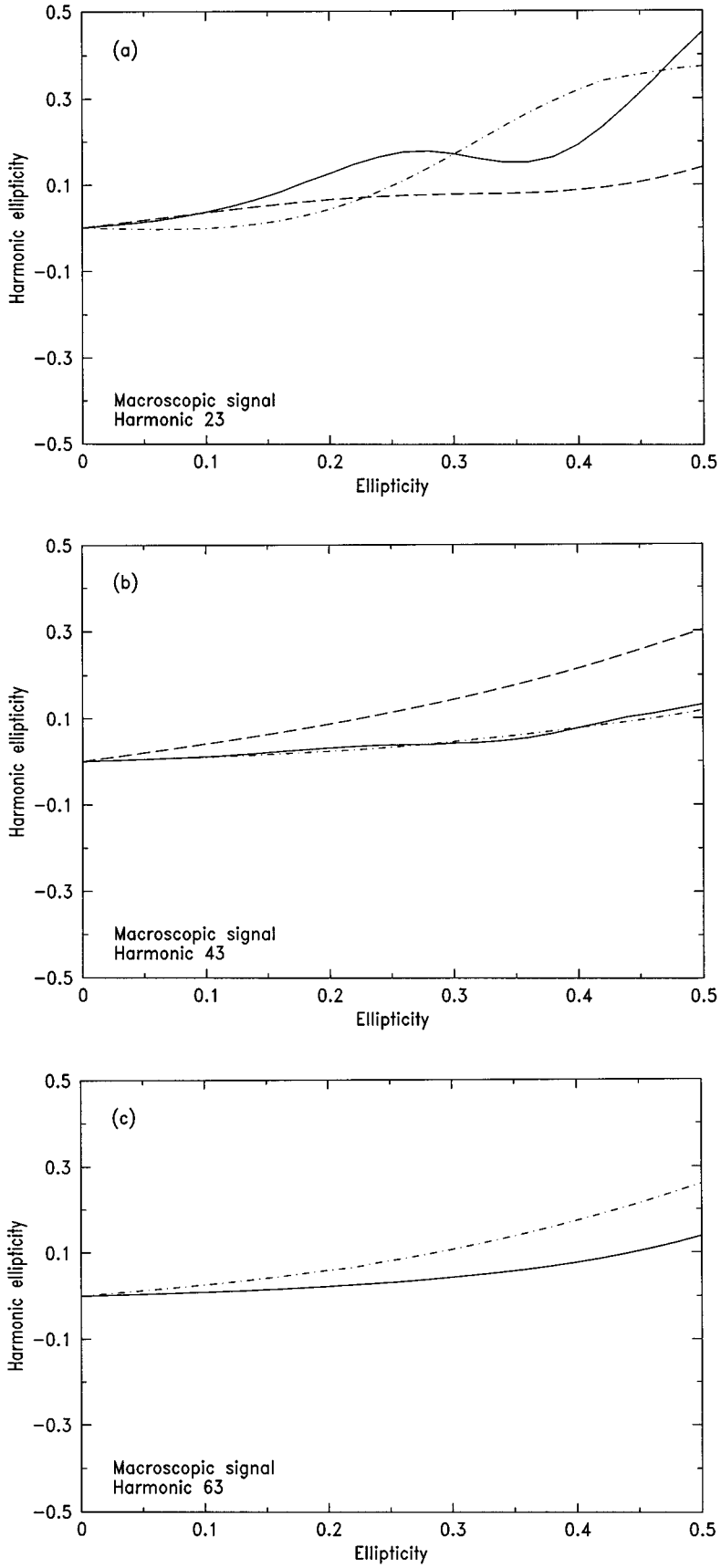

FIG. 7. Same as Fig. 6 but for the macroscopic response of the system driven by the corresponding peak intensities.

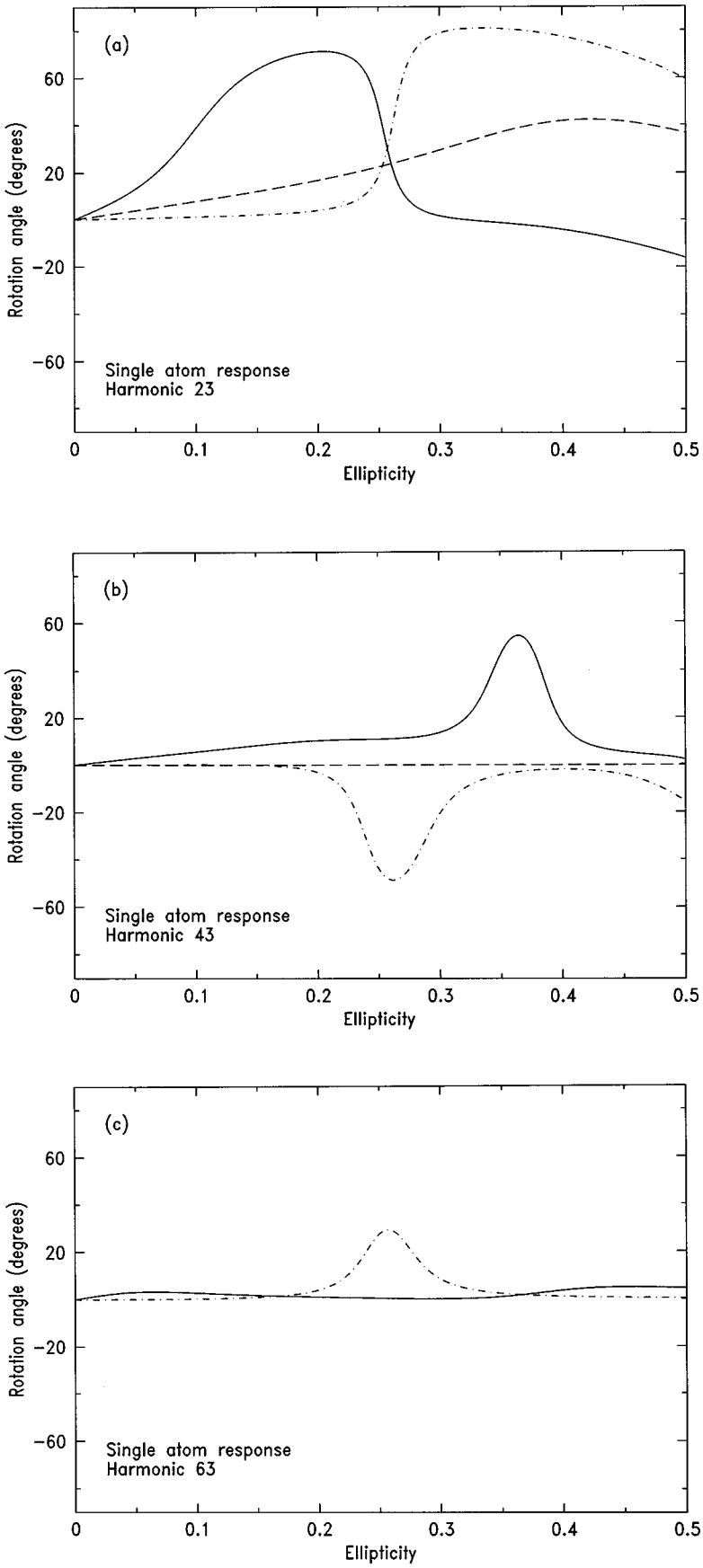

FIG. 8. Rotation angle of the harmonic ellipse with respect to the fundamental for the (a) 23rd, (b) 43rd, and (c) 63rd harmonics generated by a single atom as a function of the laser ellipticity, and for three values of the laser intensity: 2×10^{14} W/cm^2 (long-dashed line), 4×10^{14} W/cm^2 (dot-dashed line), and 6×10^{14} W/cm^2 (solid line).

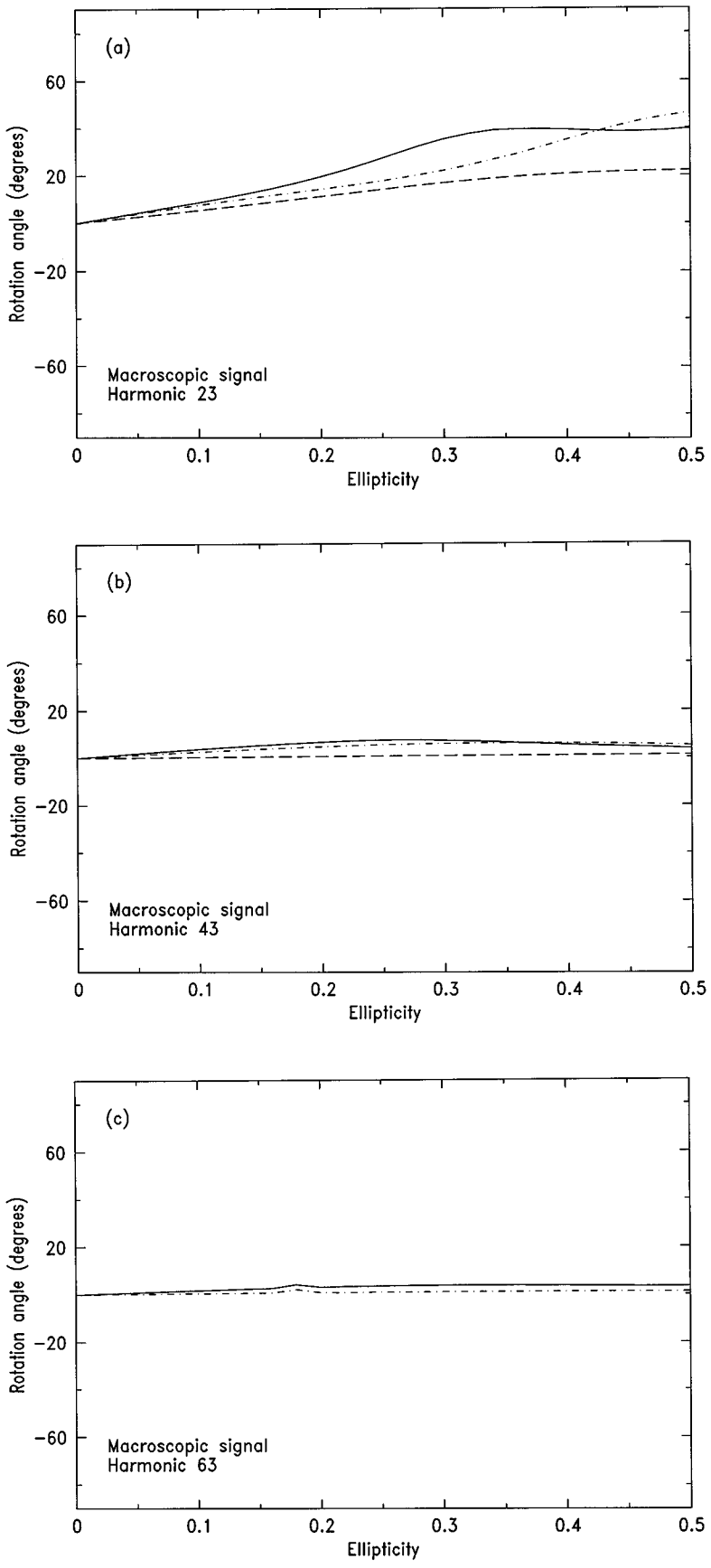

FIG. 9. Same as Fig. 8 but for the macroscopic response of the system driven by the corresponding peak intensities.

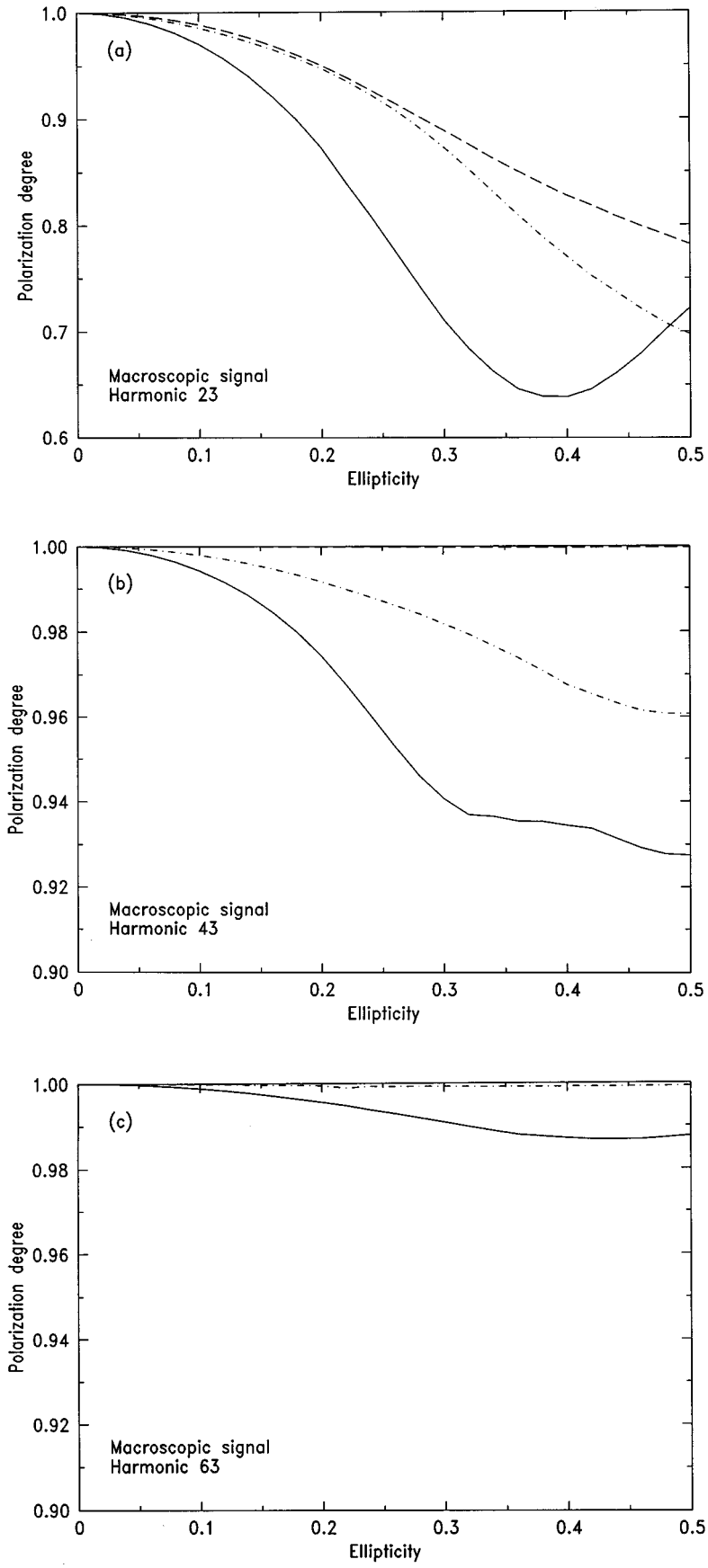

FIG. 10. Polarization degree of the (a) 23rd, (b) 43rd, and (c) 63rd harmonics as a function of the laser ellipticity, and for three values of the laser peak intensity: 2×10^{14} W/cm^2 (long-dashed line), 4×10^{14} W/cm^2 (dot-dashed line), and 6×10^{14} W/cm^2 (solid line).

$$c_M(\alpha,\tau)=\frac{1}{2\pi}\int_0^{2\pi} d[2t-\tau]e^{iM(2t-\tau)} \times\frac{1}{[\vec{p}_s(t,\tau)-\vec{A}(t-\tau)]^2+\alpha}, \tag{A1}$$

related to $b_M(\tau)$ by

$$b_M(\tau)=\frac{1}{2}\frac{\partial^2}{\partial\alpha^2}c_M(\alpha,\tau)\Big|_{\alpha=2I_p}. \tag{A2}$$

Introducing the complex variable $z=e^{i(2t-\tau)}$, the integral (47) reduces to a contour integral along the unit circle $\mathscr{C}$,

$$c_M(\alpha,\tau)=\frac{1}{2\pi i}\int_{\mathscr{C}} dz\,\frac{z^M}{W_1(\alpha,\tau)z+V(\tau)z^2+V^*(\tau)}, \tag{A3}$$

where

$$W_1(\alpha,\tau)=2U_p[a^2(\tau)+s^2(\tau)]+\alpha, \tag{A4}$$

$$V(\tau)=[W_2(\tau)-iW_3(\tau)]/2, \tag{A5}$$

$$V^*(\tau)=[W_2(\tau)+iW_3(\tau)]/2, \tag{A6}$$

$$W_2(\tau)=2\tilde{U}_p[s^2(\tau)-a^2(\tau)], \tag{A7}$$

$$W_3(\tau)=-4\tilde{U}_p a(\tau)s(\tau), \tag{A8}$$

with $s(\tau)=\sin(\tau/2)$, $a(\tau)=\cos(\tau/2)-2\sin(\tau/2)/\tau$.

For $M\geqslant 0$, we obtain

$$c_M(\alpha,\tau)=\frac{z_1^M(\alpha,\tau)}{\sqrt{W_1^2(\alpha,\tau)-W_2^2(\tau)-W_3^2(\tau)}}, \tag{A9}$$

with

$$z_1(\alpha,\tau)=(-W_1(\alpha,\tau)+\sqrt{W_1^2(\alpha,\tau)-W_2^2(\tau)-W_3^2(\tau)})/2V(\tau), \tag{A10}$$

From Eqs. (48) and (55), the analytic expression for $b_M(\tau)$ can be easily obtained. For $M<0$, we use $b_{-M}(\tau)=b_M^*(\tau)$.

APPENDIX B: ADDITIONAL DEFINITIONS

In this appendix, we present the explicit expressions for the functions $C(\tau)$, $B(\tau)$, $D(\tau)$, and $F_K(\tau)$ that enter the expressions (20) and (21). Their definitions are, in fact, the same as for the case of the GBR discussed in [9]. These functions are given by

$$C(\tau)=\sin(\tau)-\frac{4\sin^2(\tau/2)}{\tau}, \tag{B1}$$

$$B(\tau)=-\frac{2\sin^2(\tau/2)}{\tau^2}+\frac{\sin(\tau)}{\tau}-\frac{1}{2}, \tag{B2}$$

$$D(\tau)=-2B(\tau)-1+\cos(\tau), \tag{B3}$$

$$F_K(\tau)=(I_p+U_p-K)\tau-\frac{4U_p\sin^2(\tau/2)}{\tau}. \tag{B4}$$

[1] J. J. Macklin, J. D. Kmetec, and C. L. Gordon III, Phys. Rev. Lett. **70**, 766 (1993); A. L'Huillier and Ph. Balcou, *ibid.* **70**, 774 (1993).

[2] K. C. Kulander, K. J. Schafer, and J. L. Krause, in *Super-Intense Laser-Atom Physics*, Vol. 316 of *NATO Advanced Study Institute, Series B: Physics*, edited by B. Piraux, Anne L'Huillier, and K. Rzążewski (Plenum, New York, 1993), p. 316.

[3] P. B. Corkum, Phys. Rev. Lett. **71**, 1999 (1993).

[4] J. L. Krause, K. J. Schafer, and K. C. Kulander, Phys. Rev. Lett. **68**, 3535 (1992).

[5] L. V. Keldysh, Zh. Éksp. Teor. Fiz. **47**, 1945 (1964) [Sov. Phys. JETP **20**, 1307 (1965)]; F. Faisal, J. Phys. B **6**, L312 (1973); H. R. Reiss, Phys. Rev. A **22**, 1786 (1980).

[6] M. V. Ammosov, N. B. Delone, and V. P. Kraïnov, Zh. Éksp. Teor. Fiz. **91**, 2008 (1986) [Sov. Phys. JETP **64**, 1191 (1986)]; N. B. Delone and V. P. Kraïnov, J. Opt. Soc. Am. B **8**, 1207 (1991); V. P. Kraïnov and V. M. Ristić, Zh. Éksp. Teor. Fiz. **101**, 1479 (1992) [Sov. Phys. JETP **74**, 789 (1992)].

[7] It is worth stressing here that this model describes well harmonic generation for (a) low-frequency lasers, (b) high-order harmonics, and (c) not too high intensities. It does not work particularly well for KrF lasers, see J. B. Watson, A. Sanpera, and K. Burnett, Phys. Rev. A **51**, 1458 (1995); it does not seem to work for harmonic orders comparable to I_p, see N. H. Burnett, C. Kan, and P. B. Corkum, Phys. Rev. A **51**, R3418 (1995); it fails apparently when depletion of the atomic ground state is very fast and occurs via overbarrier ionization, P. Moreno, L. Plaja, V. Malyshev, and L. Roso, Phys. Rev. A **51**, 4746 (1995).

[8] A. L'Huillier, M. Lewenstein, P. Salières, Ph. Balcou, M. Yu. Ivanov, J. Larsson, C. G. Wahlström, Phys. Rev. A **48**, R3433 (1993).

[9] M. Lewenstein, Ph. Balcou, M. Yu. Ivanov, Anne L'Huillier, and P. Corkum, Phys. Rev. A **49**, 2117 (1994).

[10] W. Becker, S. Long, and J. K. McIver, Phys. Rev. A **50**, 1540 (1994), and references therein.

[11] P. Salières, A. L'Huillier, and M. Lewenstein, Phys. Rev. Lett. **74**, 3776 (1995).

[12] M. Lewenstein, P. Salières, and A. L'Huillier, Phys. Rev. A **52**, 4747 (1995).

[13] The role of the intensity-dependent induced atomic phase has been addressed in several papers: Macklin *et al.* notice it in Ref. [1]; Rae *et al.* discuss the related delay between the maxima of the fundamental field and the maxima of the harmonic emission [S. C. Rae, K. Burnett, and J. Cooper, Phys. Rev. A **50**, 3438 (1994)]; the influence of the phase on the angular distribution of harmonics is discussed by J. E. Muffet,

C.-G. Wahlström, and M. H. R. Hutchinson, J. Phys. B **27**, 5693 (1994), and J. Peatross, M. V. Fedorov, and K. C. Kulander, J. Opt. Soc. Am. B **12**, 863 (1995); the influence of the phase on temporal and spectral properties of the harmonics is presented in C. Kan, C. Capjack, R. Rankin, and N. H. Burnett, Phys. Rev. A **52**, R4336 (1995).

[14] K. S. Budil, P. Salières, Anne L'Huillier, T. Ditmire, and M. D. Perry, Phys. Rev. A **48**, R3437 (1993).

[15] P. Dietrich, N. H. Burnett, M. Yu. Ivanov, and P. B. Corkum, Phys. Rev. A **50**, R3585 (1994).

[16] Y. Liang, M. V. Ammosov, and S. L. Chin, J. Phys. B **27**, 1296 (1994).

[17] N. H. Burnett, C. Kan, and P. B. Corkum, Phys. Rev. A **51**, R3418 (1995).

[18] N. L. Manakov and V. D. Ovsyannikov, Zh. Éksp. Teor. Fiz. **79**, 1769 (1980) [Sov. Phys. JETP **52**, 895 (1980)].

[19] F. A. Weihe, S. K. Dutta, G. Korn, D. Du, P. H. Bucksbaum, P. L. Shkolnikov, Phys. Rev. A **51**, R3433 (1995).

[20] P. B. Corkum, N. H. Burnett, and M. Y. Ivanov, Opt. Lett. **19**, 1870 (1994).

[21] M. Yu. Ivanov, P. B. Corkum, T. Zuo, and A. Bandrauk, Phys. Rev. Lett. **74**, 2933 (1995).

[22] H. Eichmann, A. Egbert, S. Nolte, C. Momma, B. Wellegehausen, W. Becker, S. Long, and J. K. McIver, Phys. Rev. A **51**, R3414 (1995).

[23] Anne L'Huillier, Ph. Balcou, S. Candel, K. J. Schafer, and K. C. Kulander, Phys. Rev. A **46**, 2778 (1992).

[24] N. B. Delone and V. P. Kraïnov, *Atoms in Strong Fields* (Springer-Verlag, Heidelberg, 1985); L. D. Landau, *Quantum Mechanics* (Pergamon, New York, 1964).

[25] F. Brunel, J. Opt. Soc. Am. B **7**, 521 (1990).

[26] H. A. Bethe and E. E. Salpeter, *Quantum Mechanics of One and Two Electron Atoms* (Academic, New York, 1957).

[27] In particular, we have compared the ionization rates of helium as obtained from (a) the exact numerical solution of Schrödinger equation, (b) the theory of Ref. [6], (c) our theory using Eq. (15), and finally (d) the GBR model. The curves obtained from both (b) and (c) are typically a factor 1.5–2 times smaller than (a) in the considered regime of intensities ($\leqslant 10\times 10^{15}$ W/cm^2). The results (d) normalized as discussed in Sec. II are 2–3 orders of magnitude smaller than (a); Ph. Antoine, K. C. Kulander, A. L'Huillier, and M. Lewenstein (unpublished).

[28] Ph. Antoine and B. Carré (unpublished)

[29] Y. R. Shen, *The Principles of Nonlinear Optics* (Wiley, New York, 1984).

[30] C. Altucci, T. Starczewski, B. Carré, A. L'Huillier, and C.-G. Wahlström, J. Opt. Soc. Am. B (to be published).

[31] M. Born and E. Wolf, *Principles of Optics* (Pergamon, New York, 1964).